Saph Pani

Enhancement of natural water systems and treatment methods for safe and sustainable water supply in India

Project supported by the European Commission within the Seventh Framework Programme Grant agreement No. 282911

Deliverable 3.2

Conceptual model of flow and transport for a hard rock aquifer – Musi River micro-watershed case study

SAPHPANI

Work package	WP3 - Constructed wetlands and other Natural treatment systems for wastewater Treatment and reuse
Deliverable number	D 3.2
Deliverable title	Report on Conceptual model of flow and transport for a hard rock aquifer – Musi River micro-watershed case study, Andhra Pradesh
Due date	M24
Actual submission date	M30
Start date of project	01.10.2011
Participants (Partner short names)	IWMI (Lead), NGRI and BRGM
Authors in alphabetic order	Shakeel Ahmed (CSIR-NGRI), Marina Alazard (BRGM), Priyanie Amerasinghe (IWMI), Alexandre Boisson (BRGM), Jampani Mahesh (IWMI), Paul Pavelic (IWMI), Sahebrao Sonkamble (CSIR-NGRI)
Contact for queries	Priyanie Amerasinghe E-mail: p.amerasinghe@cgiar.org Address: International Water Management Institute, 401/5, IWMI, ICRISAT Campus, Patancheru, Telangana, Hyderabad – 502 324, India. Phone: +91 40 3071 3745
Dissemination level: (public, Restricted to other Programmes Participants, restricted to a group specified by the consortium, confidential- only for members of the consortium)	PU
Deliverable Status:	Revision 3.0

Content

List of figures

List of tables

1 Introduction

This deliverable describes a conceptual model of flow and transport for a hard rock aquifer, based on studies carried out in a micro-watershed of the Musi river, and discusses the natural treatment processes that may be involved in contaminant attenuation.The Musi River a tributary of the Krishna River receives large volumes of both untreated and partially treated wastewater from the city of Hyderabad, as such, wastewater irrigation is a common practice along the banks of the river. The river water is channelled via irrigation canals, or lifted via pumps for agriculture production. Where wastewater is not accessible groundwater is utilised for crop production. As such, a complex system of irrigation practices exists within the catchment, especially in areas where agriculture production is practiced.

A number of studies on the Musi River catchment have dealt with water quality and hydrology (Perrin et al., 2011; Schmitt, 2010; Amerasinghe et al., 2009) livelihood opportunities (Buechler et al., 2002), salinity implications (Mccartney et al., 2008; Biggs and Jiang, 2009) water quality and health risks (Ensink et al., 2008) and contamination remediation through irrigation infrastructure (Ensink et al., 2010). However, studies on the impact of wastewater irrigation on ground water and the natural treatment processes that attenuate contamination in the peri-urban areas of this catchment, has not been investigated.

This deliverable describes the investigations that led to the development of a conceptual model of flow and transport of a hard rock aquifer, and comments on the natural treatment processes that may be involved in contaminant attenuation. The numerical modelling for the same catchment is described in Work Package 5 (WP5). In order to develop a conceptual model of flow and transport for the local hard-rock aquifer system and understand the impact of wastewater on ground water, the following activities were carried out:

- Literature review of studies carried out in the catchment
- Land use surveys
- River discharge measurements
- Water level monitoring (continuous and piezometric campaigns)
- Water budgeting
- Pumping tests
- Geophysical surveys (Electrical resistivity tomography)
- Water quality analysis (major ions, trace elements, microbiology and pesticides) – only the major ions were considered to develop the conceptual model

2 Site Characterization

The Musi River is a small tributary of the Krishna River and its basin constitutes approximately 4% of the total Krishna River basin. The river originates from the Ananthagiri hills and passes through the city of Hyderabad and finally reaches the Krishna River at Wazirabad (Figure 1). Its total length is 247 km. After it leaves the city, the water is impounded by weirs (n=22) at various sections, allowing the water to be extracted for agriculture via a series of irrigation canals (Ensink et al., 2010). Currently an estimated 1.2 million m^3/day of wastewater (both domestic and industrial) is funnelled into the river, which is a mixture of partially treated or untreated water. The wastewater is a significant

resource in this semi-arid peri-urban environment, where the cultivation of fodder grass, paddy and vegetables provides economic benefits to many inhabitants. Year round cultivation, which generates large return flows from irrigated fields, contributes to a large share of the aquifer recharge (Dewandel et al., 2008). Shallow groundwater is also pumped locally for irrigation on terrains where canal water is not accessible, or where it is too polluted for certain crops according to farmers, especially paddy rice. The irrigation canals that run parallel to the river end in a storage tank, serving many rural communities. Canal discharge rates are highly variable in space and time, and generally considered to be low (less than 2 m^3/s).

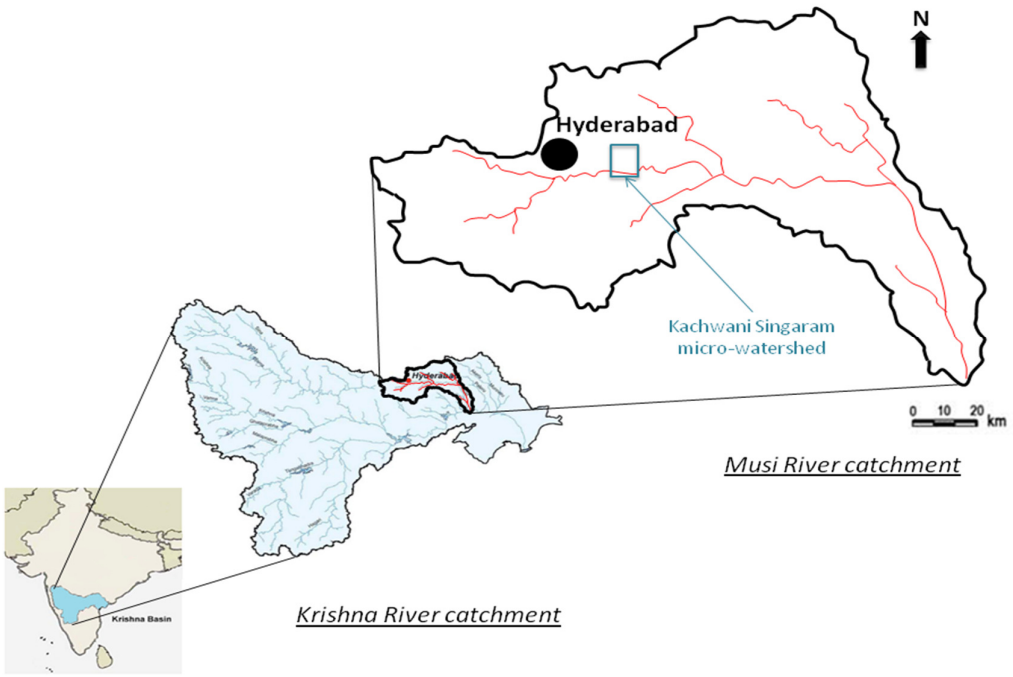

Figure 1 The Kachwani Singaram micro-watershed in the Musi River sub-basin, Telangana, India

The micro-watershed Kachiwani Singaram (KSMWS), is a periurban site in the Musi river catchment comprising an area of 2.74 km^2 (Figure 2). The irrigation water supply is via an irrigation canal positioned at the first weir in the river, which is situated at Peerzadiguda. The canal runs approximately 14 km and ends in a village tank, supporting many livelihoods on its way.

The Musi riverbed shows a flat topography (mean slope < 1%) (Massuel et al., 2007). Aerial photography and digital elevation model of the KSMWS are presented in Figure 3. The area has a semi-arid climate with a mean annual rainfall of 750 mm, with both high spatial and temporal variability. The annual rainfall in Hyderabad for the years 2000 and 2011 varied from 535 to 1473 mm respectively (Figure 4). Most of the rain events occur during the monsoon period from June to September. The mean annual temperature is about 26 °C, although during the summer time the maximum temperature can reach up to 45 °C.

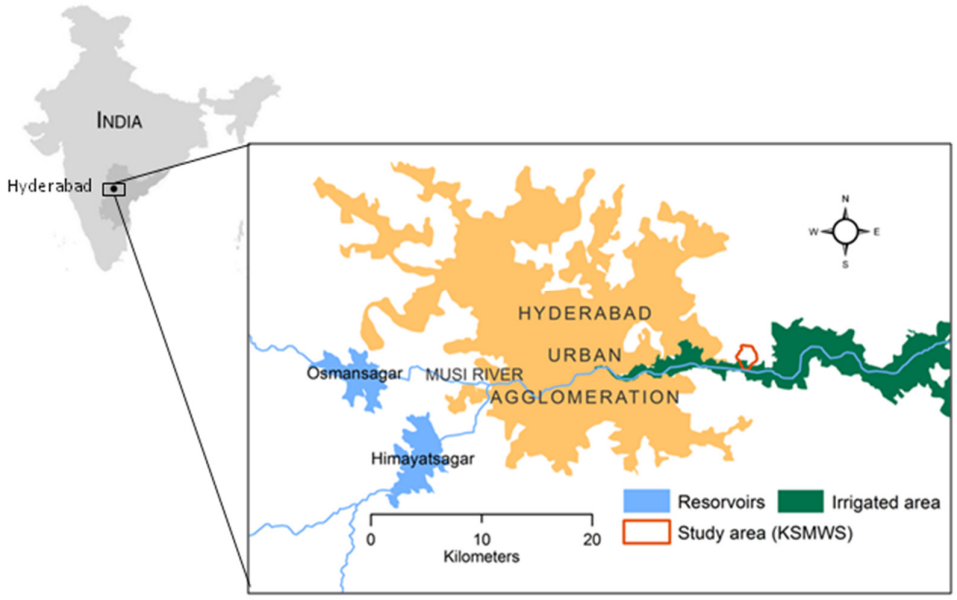

Figure 2 Location map of Kachiwani Singaram micro-watershed

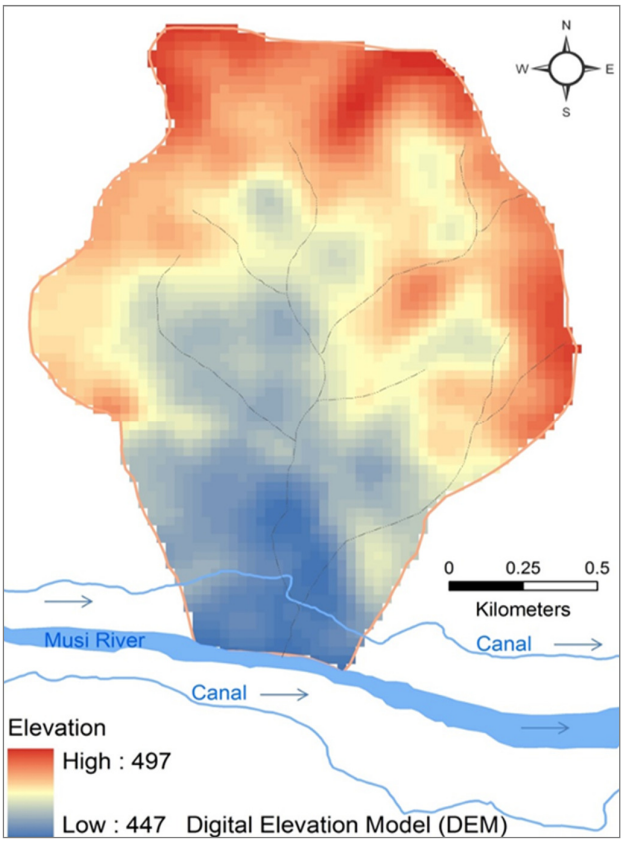

Figure 3 Digital elevation map of the Kachwani Singaram micro-watershed

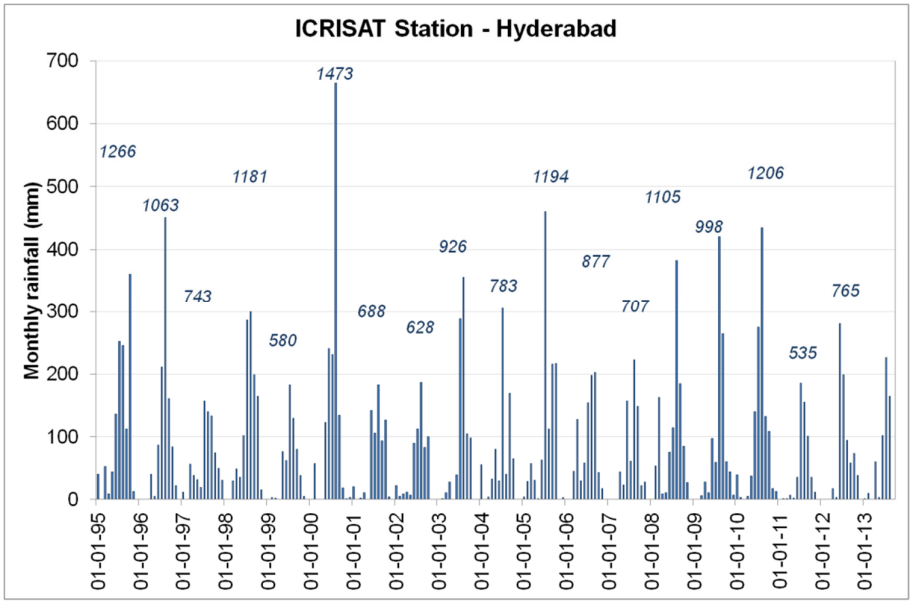

Figure 4 Rainfall pattern in Hyderabad: monthly rainfall from 1995 to 2013. Annual average is given in italics (Source: ICRISAT, internal data base accessed in December 2013)

3 Materials and Methods

3.1 Land-use land-cover estimations

Land use mapping was carried out using high resolution satellite imagery (Google Earth) and digital globe satellite data (accessed on January 21st, 2012), which was validated with field observations and farmer interviews. The data sets were also Geo-referenced using UTM projection and WGS 84 datum. The datasets on cropping patterns, built-up area, topographical maps, and farmer interviews were used as inputs for classification and accuracy assessment. The spatial variability of cropping patterns and other land cover classes were estimated using the same data sets and imagery.

3.2 Surface water

River discharge data collected in 2007-2008 were used in this study. The method used was a simple float method, where an orange was allowed to travel a 50 foot distance in the canal or river that was free of vegetation. The time taken to travel the distance was noted. If the flow was very slow, shorter distances were considered. The procedure was repeated three to five times at a particular site and the average was used in the analysis. The location of river discharge measurements and water sampling points is presented in Figure 5 and associated canals discharge measurement points and sampling points at corresponding villages are shown in Figure 6.

Since the flat topography and the urbanization may lead to a complex surface flow in the micro-watershed, surface modeling based on topography was performed using ArcGIS software. Topography was estimated from the ASTER DEM with 30 m resolution datasets.

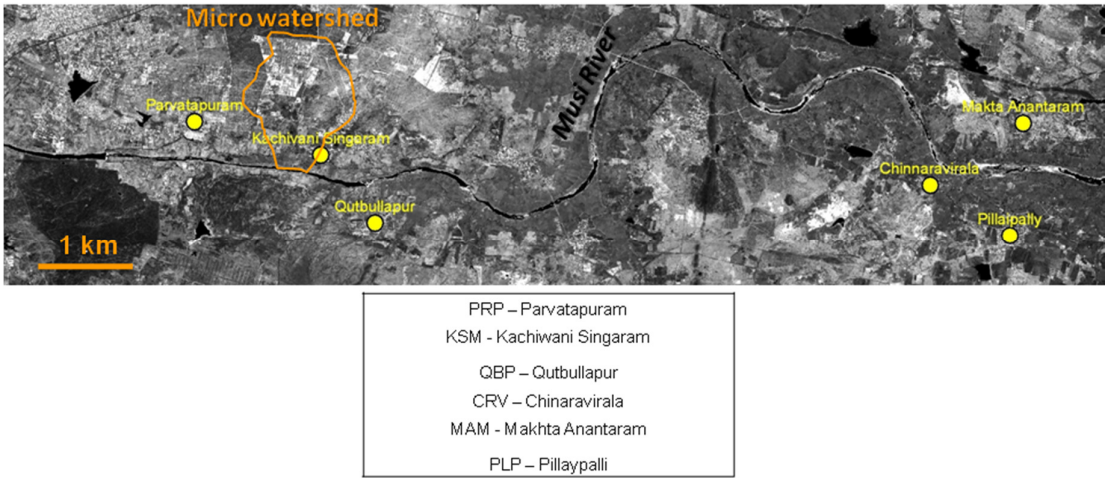

Figure 5 Location of the discharge measuring points in the villages along the Musi River

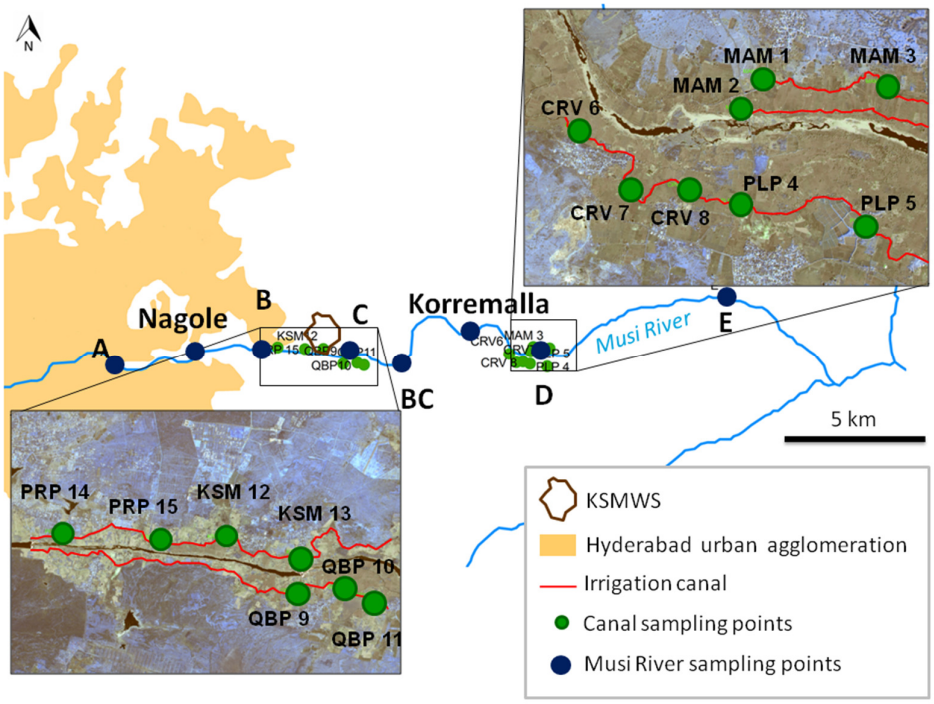

Figure 6 Location of the Musi River and associated canal discharge measurement points (River and canal sampling points A, B, C, BC, D and E (2006-2008) and PRP 14 and 15; KSM 12 and 13; QBP 9, 10 and 11; CRV 6, 7 and 8; MAM 1, 2 and 3; PLP 4 and 5 (2007/2008)

3.3 Geophysical Investigations

Electrical resistivity tomography (ERT) survey was carried out to delineate the deposition of the subsurface lithological layers and saturated thickness. SYSCAL Junior Switch multi-node computer-controlled imaging system (IRIS make, France) was used with 48 electrodes connected to the multi-core cable. Wenner–Schlumberger and Dipole-Dipole configurations were opted to scan the subsurface for the profile length ranging from 96 to 470 m (as per the availability of space) with unit electrode spacing 2.0 m to 10.0 m.

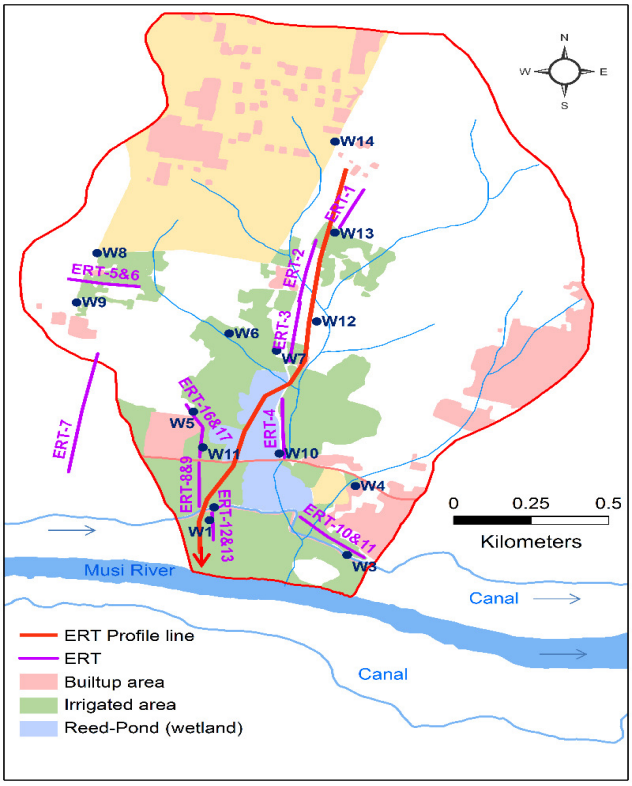

Figure 7 Geophysical measurement (ERT) locations in the Kachiwani Singaram micro-watershed

Each electrode was watered to ensure good contact with the ground. This was done most effectively by withdrawing the electrode from the ground, and filling the hole with water and replanting the electrode. A total of 17 ERT profiles was carried out at 11 different locations (Figure 7) to capture the various stages of weathering processes. A continuous ERT profile line A-A| of 1.62 Km distance was chosen to decipher the spatial variations of regolith (saprolite) thickness and saturated zone, and also to determine subsurface contamination from north to south orientation up to the Musi River. In addition to the A-A| profile line, the ERT investigations were also performed at other locations in the proximity of observation wells. Detailed information encompassing site geology, geomorphological and hydrogeological conditions at each ERT profile was noted down during the ERT investigations which was useful in the geophysical image interpretation.

3.4 Geophysical Investigations

Monthly measurements of water levels were carried out in the four monitoring piezometers drilled in 2009 by BRGM (MU01 = W1, MU02 = W5, MU03 = W8 and MU04 = W6, Figure 8)[1]. The W1 well was positioned south of the irrigation canal in a paddy field and captured a wastewater contaminated shallow unconfined aquifer. W5 was located 400 m north of the irrigation canal and was in a paragrass field irrigated with wastewater. W6 was at 700 m north of the irrigation canal, located in a paddy field irrigated with groundwater. Similarly, W8 was 1 km north of irrigation canal, and positioned at an elevated topography, located in a vegetable farmland irrigated with groundwater.

[1] The well numbering of the wells were changed to a W series during 2012 campaigns

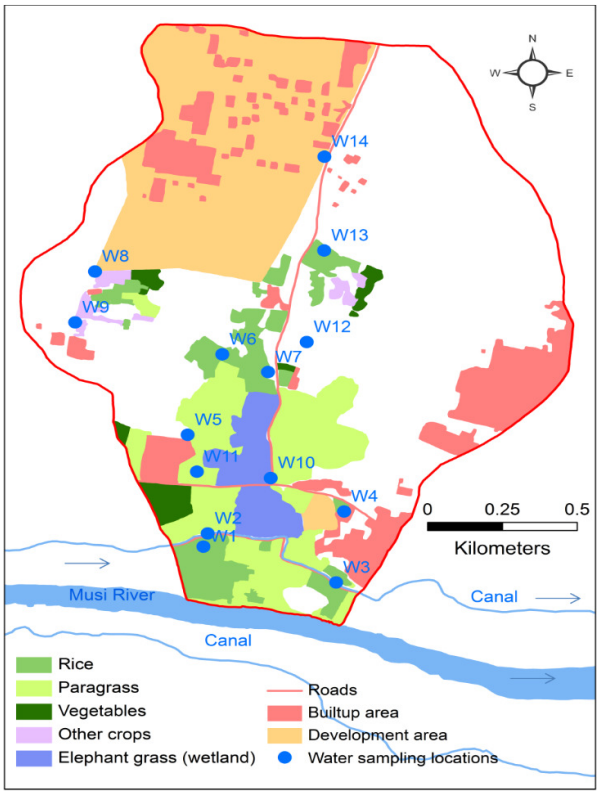

Figure 8 Surface and ground water sampling points (W1-W14) and land use classes in the Kachiwani Singaram micro-watershed

Water levels and temperature were monitored daily at 30 minute intervals in W6 and W8, using Automatic level-loggers (Solinst® Levelogger). Automatic monitoring in W6 commenced in 2010, however, had to be uninstalled due to mechanical failure.

Four extended piezometric campaigns were carried out in May, June (pre-monsoon), September (monsoon), and October (post-monsoon) of 2010. Through interpolation using inverse distance weighting (IDW), annual (pre- / post- monsoon 2010) and inter-annual comparison (post- monsoon 2010 / post-monsoon 2013) maps were computed and further analyzed to highlight particular patterns of levels of groundwater.

Hydrodynamic properties were assessed by conducting hydraulic tests, i.e. Pumping test, in the four piezometers (W1, W5, W8 and W6). The drawdown was monitored during the entire pumping duration (recorded at 1 min intervals). Then the recovery was recorded every minute up to reaching the initial water level. These data were used to estimate hydrodynamic characteristics of the aquifer using the software winisape© developed by BRGM. The Theis method was used for interpretation (Theis 1935). A best-fitting procedure led to the computation of the transmissivity parameter.

Variations of water velocity inside the bore well was measured during pumping. A flow meter with a propeller was used for this purpose - the propeller turns when it is in contact with the water flow (measure of flow velocity). Measurements were done at the bottom of the casing and extended to the base of the hole. Each productive fissure was indicated by

a drop in flow velocity. Results were correlated with geological observations of cuttings to identify the productive zones.

3.5 Water quality

Two hydro-chemical water sampling campaigns were done in 2012 in pre monsoon (June) and post monsoon seasons (November). Sampling was done at 14 points and analyses included major anions and cations as well as pesticides. The locations of the sampling points are shown in Figure 8. The 14 sampling points include 11 groundwater, 2 canal water and 1 reed pond (wetland). Groundwater samples were from piezometers (4), tube wells (3 agriculture and 1 domestic) and open dug wells (3) (Table 1). Groundwater and surface water samples were collected in pre-cleaned one litre polyethylene sampling bottles for major cations and anions. Analysis was performed for major cations and anions as per the guidelines given in APHA, 2005[2] The pH was measured using a pH meter; electrical conductivity using a conductivity meter; carbonates, bicarbonates, calcium and magnesium using titration method; sulphate using a turbidity meter; fluoride using an ion meter; sodium and potassium using a flame photometer and nitrate using an atomic absorption spectrophotometer. Pesticides samples were collected in one litre amber coloured high density polyethylene (HDPE) bottles and kept below 4^0C until analysis. Organochlorine, Organophosphorous and Carbamate pesticides were measured using a liquid-liquid extraction method and analysed in a GC-MS (Gas chromatography – Mass Spectroscopy) instrument.

Table 1 Description of the 2012 water sampling points

Well ID	Type	Water type	Location characteristics
W1	Piezometer (MU-01)[3]	GW	Waste water irrigated rice
W2	Canal	SW/WW	Canal water
W3	Canal	SW/WW	Canal water
W4	Open well	GW	Groundwater irrigated rice
W5	Piezometer (MU-02)	GW	Waste water irrigated paragrass
W6	Piezometer (MU-04)	GW	Groundwater irrigated rice
W7	Open well	GW	Groundwater irrigated rice
W8	Piezometer (MU-03)	GW	Groundwater irrigated paragrass/vegetables
W9	Agricultural bore well	GW	Groundwater irrigated paragrass/vegetables
W10	Surface water pond	SW	Surface water pond with reeds
W11	Open well	GW	Waste water irrigated paragrass
W12	Bore well	GW	Waste water use - vermicomposting area
W13	Agricultural bore well	GW	Groundwater irrigated rice/paragrass/vegetables
W14	Domestic bore well	GW	Household bore well

[2] Water quality tests were done at National Geophysical Research Institute (NGRI), Andhra Pradesh Groundwater Department (ground water quality laboratory), KKB Microtesting Lab Pvt. Ltd. (www.**kkbmicrotestinglab**s.com), National Collateral Management Services Limited (NCML) http://www.ncmsl.com/.

[3] Well numbers in brackets refer to the number given during the 2010 sampling campaign

Results of previous sampling campaigns were used for comparison: For example, campaigns carried out in 2010 by Perrin et al. (2011) and in 2006-2008 by Amerasinghe et al. (2009), where the canal water was sampled at 6 locations (Figure 6) and Musi River was sampled at 5 locations respectively (Figure 5). These previous data sets were used to understand the groundwater dynamics in the watershed along the Musi River and also for assessing the impact of wastewater on groundwater quality.

4 Results and interpretation

4.1 Land use land cover

The land use classes in the micro-watershed are depicted in Figure 8. Built-up area refers to houses and other buildings and development areas are those that have been clearly demarcated with fencing. The irrigated area was 48 ha. According to the farmers in the area, the cropping patterns have not changed in a long time. A previous study showed that the land use pattern between 2000 and 2010 had changed only minimally (Mahesh et al., 2015). Detailed land use classification and crops grown in the irrigated land are shown in table 2.

Table 2 Land-use classification observed in the micro-watershed (year 2012)

Land-use type	Area (ha)
Built-up area	29.64
Area under development	50.20
Irrigated land	
Paragrass	27.20
Paddy rice	15.25
Vegetables	3.81
Other crops	2.27
Groundwater-irrigated area	12.66
Wastewater-irrigated area	35.87
Total irrigated area	48.53

The major crops grown in the area were paragrass (56%), paddy rice (32%) and vegetables (8%). 74% of the total area were under wastewater irrigation, and the remainder was irrigated with groundwater. Paragrass was the dominant crop in the watershed.

Here we considered that the minimal changes in land use will not affect the runoff parameters in the water balance. Moreover, even if more water is used for domestic purposes, it can be considered as negligible in comparison with the amount of water used for irrigation.

4.2 Surface water

4.2.1 River discharge

Water supply for the city of Hyderabad is tapped from Musi and Esa Rivers that start from the Ananthagiri hills (Figure 2). Water is stored in two tanks, namely, Himayat Sagar and Osman Sagar, which are at the head-end of the two rivers, Musi River becomes a mere trickle as it enters the city. Partially treated and untreated wastewater which is funneled into the river from the Hyderabad city, makes the river perennial, and records a current flow of greater than 1.2 milliion m^3/day (Mahesh et al., 2015). Downstream, wastewater from the river is channelized into irrigation canals for irrigation of crops. During the study period the flow rate measurement campaigns indicated an increase in irrigation rates during the wet season. Some canal discharge rates, such as that seen in the canal at Pillaipalli (September and October 2007), were as important as the river discharges (Figure 9 and Figure 10). The large volumes of wastewater from the city appeared to mask the relationship between the rainfall and river discharge (Figure 10).

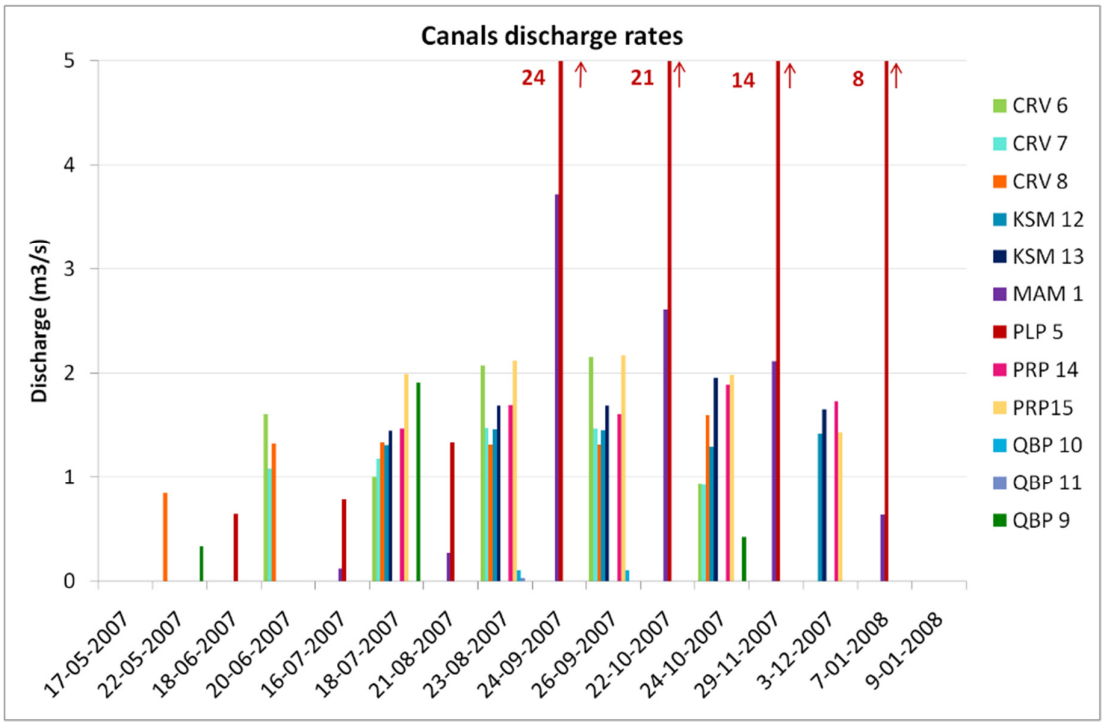

Figure 9 Discharge rate measurements in the canals during the years 2007 and 2008 (m^3/s).

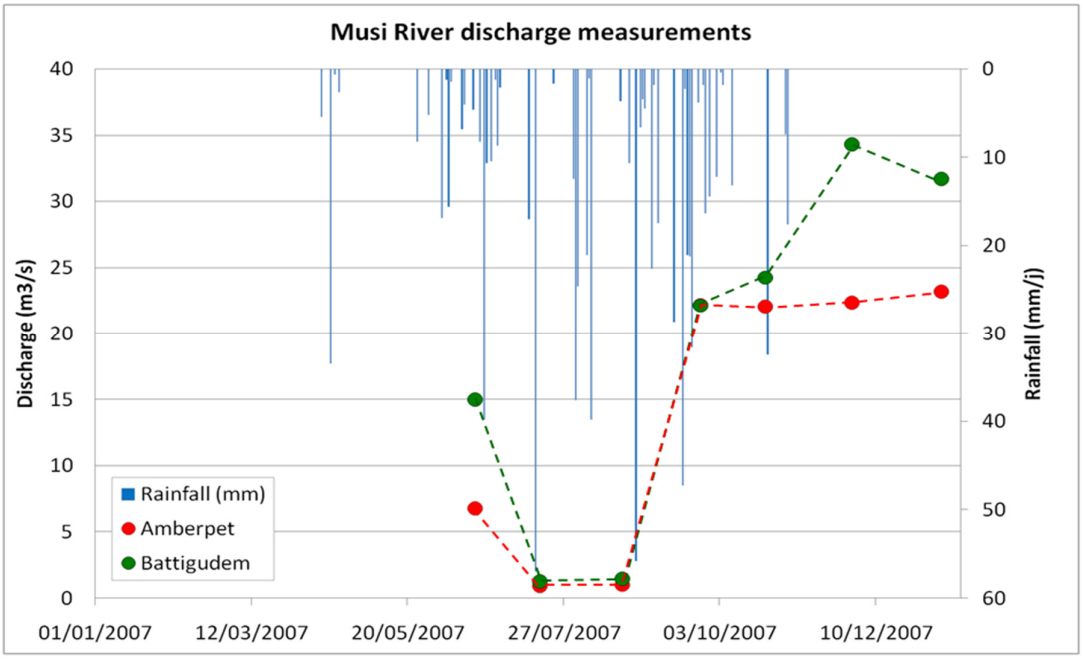

Figure 10 Discharge rate (m^3/s) measurements of the Musi River in Amberpet and Battigudem from May 2007 to January 2008 and daily rainfall (mm) in Hyderabad from January 2007 to January 2008.

4.2.2 Surface runoff

As in many semi-arid environments, spatial and temporal interactions between surface water and groundwater were complex. The surface water percolation occured mainly through preferential paths governed by topography and underground hydraulic properties. An analysis of the topography of the area using GIS tools helped to determine the main depressions and surface water flows over the micro-watershed. More than 10 small preferential flow pathways within the micro-watershed were identified (Figure 11). Local depressions can contribute to recharge, however, the major direction of the surface runoff flow was towards the canal and then into the Musi River.

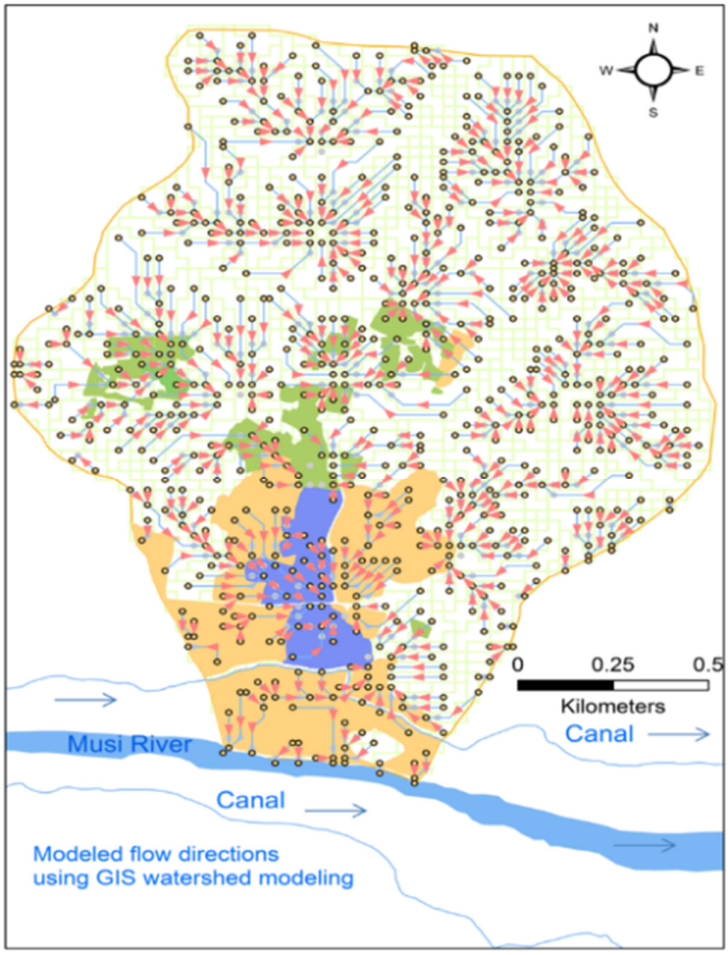

Figure 11 Watershed model showing the flow directions of Kachiwani Singaram micro-watershed.

4.3 Geology

The watershed geology was characterised by a basement made of orthogneissic granite also known as “pink granite" with granite, quartz and dolerite intrusions (Perrin et al. 2011). It consisted of large feldspars chunks and also of biotite that contributed to a generally well-developed weathering profile. The hydrogeological boundaries of the study area encompassed the surface watershed limit and extended northwards to an extensive dolerite dyke. In the western part of the watershed, significant intrusions of leucocratic granites, doleritic material and quartz/pegmatite veins constituted the main observed outcrops. Long-term weathering processes throughout the south Indian craton has led to a typical weathering profile in granitic terrains which was defined by three zones from top to bottom: (i) saprolite layer (10-15 m thick), characterized by a penetrative millimetre-spaced horizontal laminated structure and an unusual network of preserved fractures that were mainly subhorizontal and some subvertical fissures which were partially filled up by clayey minerals; (ii) a fissured layer (15-20 m); and (iii) a fresh basement where granite was unfissured (Dewandel et al., 2006) (Figure 12). Logs of the drilled boreholes followed the general description. The fracture density varied in space and decreased with depth and resulted in the compartmentalization of the aquifer system in this granitic hard rock (e.g.Chandra et al., 2006; Chandra et al., 2008 Dewandel et al., 2006; Guihéneuf et al., 2014).

Thus, from the hydrogeological point of view, the most important layers were the saprolite and fissured layers which made up a double layer system with their respective hydrodynamic properties. The saprolite layer was of a clayey-sandy composition with a significant porosity but quite low in permeability. This layer had part of the storage capacity of the aquifer when it was saturated. The fissured layer, due to its horizontal fissuring network, constituted the main transmissive zone of the aquifer (Marechal et al., 2006). Examples of outcrops are presented Figure 12.

The Geomorphology of the study area is shown in Figure 13 and table 3. Potential recharge conditions varied from poor to good from north to south of the micro-watershed.

Figure 12 Field specimens showing the (a) weathered quartz pegmatite vein(b) weathered quartz with granite outcrops (c) quartz vein intrusion (d) outcrops of granite

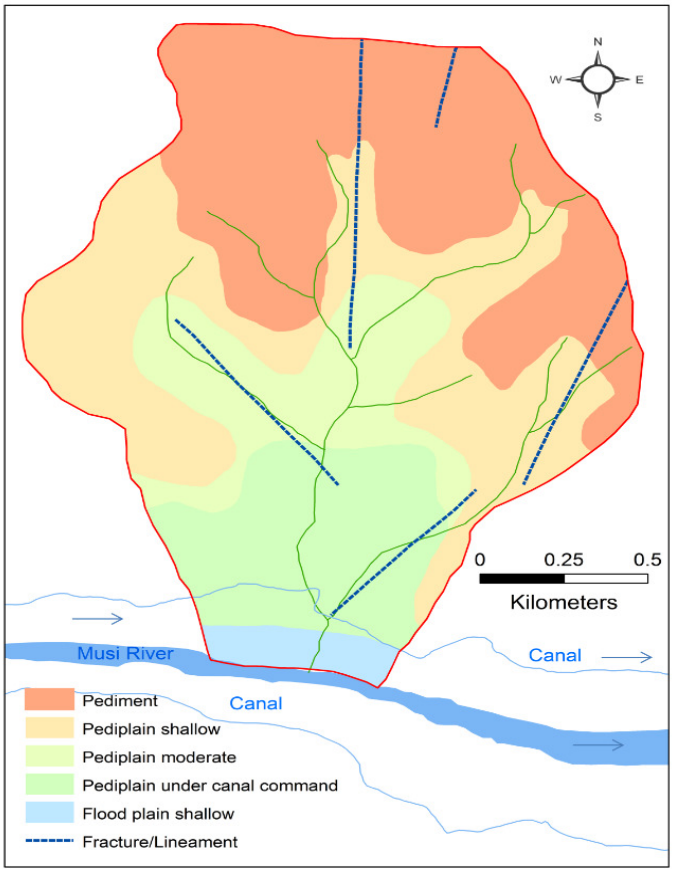

Figure 13 Geomorphology of the Kachiwani Singaram micro-watershed

Table 3 Geomorphology and potential ground water recharge conditions

Geological Sequence	Rock Type	Geomorphic form/ Landform	Potential recharge conditions
Archean	Granite	Pediment	Poor
	Migmatite	Pediplain shallow	Moderate
	Granite Gneiss	Pediplain under canal command	Good
	Migmatite	Pediplain moderate	Moderate
	Granite	Floodplain shallow	Good

4.4 Geophysical studies

The ERT survey profiles were carried out at many locations. The first was designated as A-A$^{|}$ line and was established keeping the 1st electrode towards north and 48th towards the south. The elevation of the A-A$^{|}$ profile line varied from 485 m above mean sea level (AMSL) in the north to 461 m AMSL in the south therefore, indicated an elevation gradient of 24 m for 1620 m distance (Figure 14).

In addition to the A-A$^{|}$ profile line, the ERT investigations were also performed at other locations in close proximity of the observation wells. Here we present the results of the A-A$^{|}$ profile line as an example. A number of other ERT profiles were also developed within the micro-watershed to understand the geophysical layout.

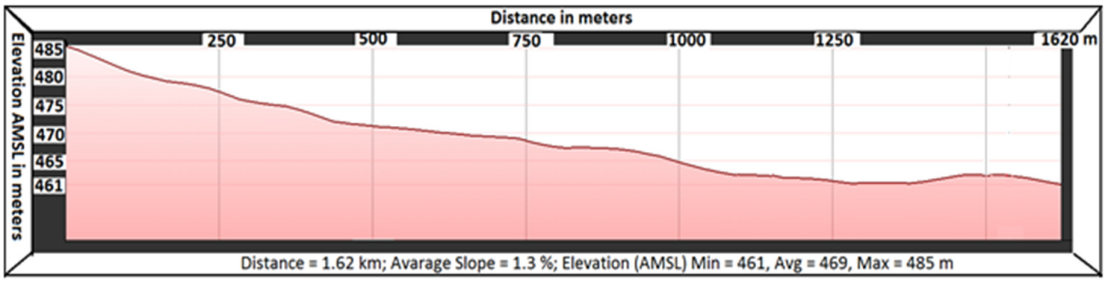

Figure 14 Elevation (AMSL) at A-A| line of the Kachiwani Singaram micro-watershed (Source of elevation data: Google Earth).

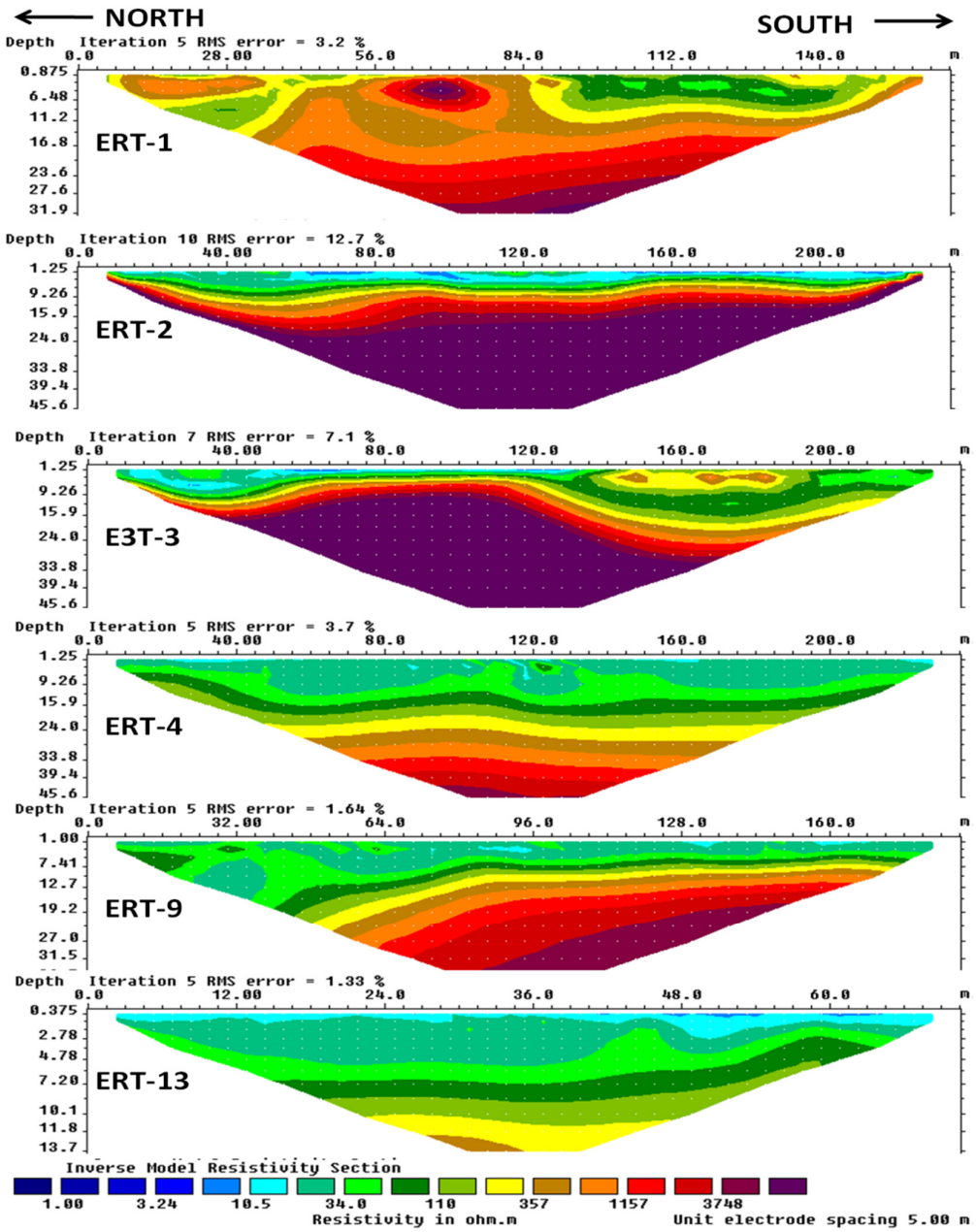

Figure 15 ERT profile line of A-A| in N-S orientation of the Kachiwani Singaram micro-watershed

The ERT profile line A-A' indicated the variations in regolith thickness from north to south orientation. The profile line of 1620 m length covered the ERT numbers 1, 2, 3, 4, 8, 9, 12 and 13 among which 8 and 12 were Dipole-Dipole configuration and the rest were Wenner-Schlumberger configuration (Figure 15). Dipole-Dipole array was useful to detect a conductive layer at the shallow sub-surface, therefore, it was performed at locations close to the Musi River, where the contamination was also assumed to be higher. The inverse model resistivity sections of all the ERT profiles indicated a wide range of electrical resistivity at vertical and lateral scales, which is typical of crystalline aquifer heterogeneity (Figure 16).

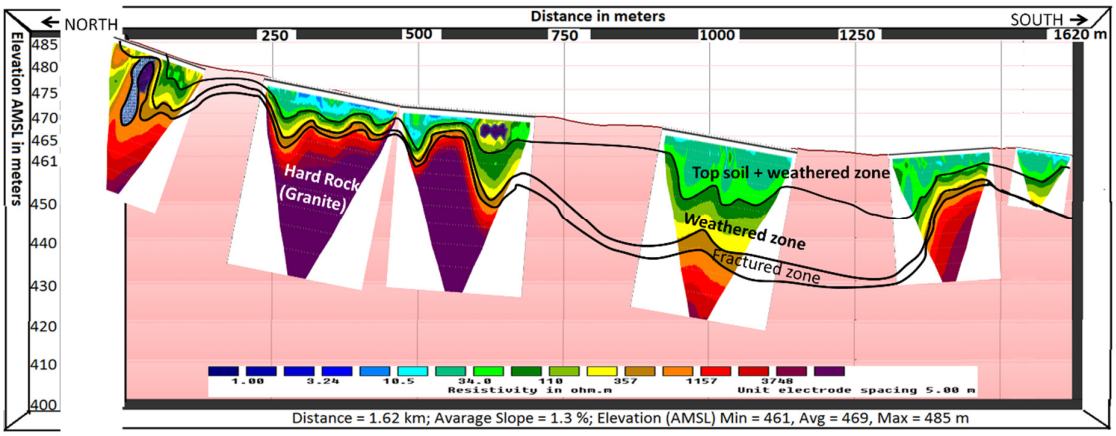

Figure 16 Geo-electrical layers cross section (referenced to MSL) derived from A-A' ERT data of N-S profile at the Kachiwani Singaram micro-watershed

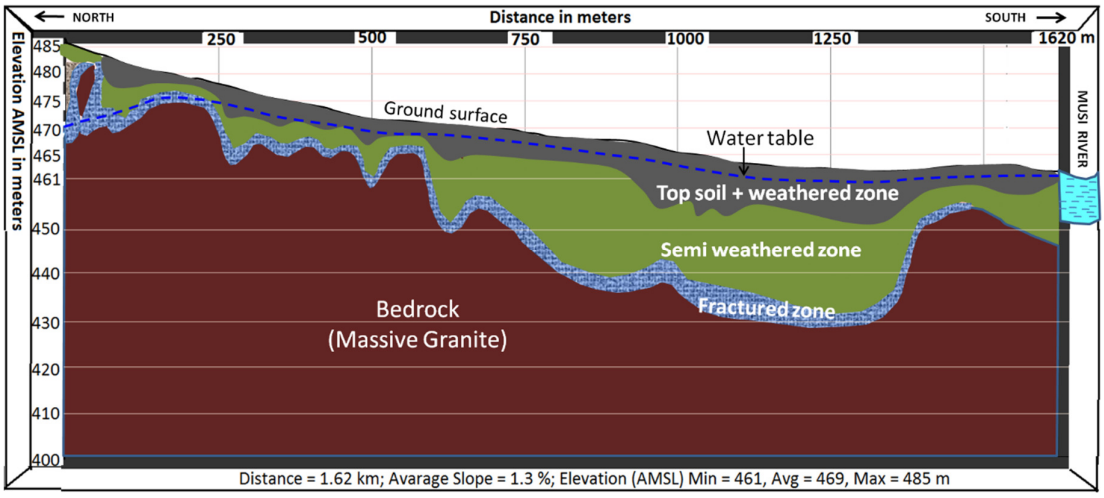

Figure 17 Geological cross section with the altitude derived from A-A' ERT data of N-S profile at the Kachiwani Singaram micro-watershed

The geological cross section based on ERT data indicated considerable variations in the regolith (weathered formation over the base rock) thickness from north to south orientation (Figure 17). Regolith constituted the top loose soil, weathered granite gneiss; semi

weathered and fractured granite gneiss which possessed different resistivity ranges. At the northern end of the profile line, the out crops (granite) were noted.

The electrical resistivity of the top soil and weathered zone ranged from 10 to 70 Ω-m. The maximum thickness of top soil and weathered zone was attained at the wetland (W10) due to the chemical weathering. Here, a low resistivity range from 10-35 Ω-m indicated a conductive saturated zone with possible contamination up to 15 m depth from the ground surface. The water level measured along the profile is shown in Figure 17 which appears to follow the topography. Further, the gentle raise in topographic elevation towards the Musi River, causes thinning of weathered layer up to 4 m depth. The beneath the weathered zone was a semi weathered zone with a resistivity range 100-300 Ω-m. The semi-weathered zone was of uneven thickness, but at the midpoint tapering towards the river it gained the highest depth. The fractured layer that was next to semi-weathered zone was of ~1-5 m thickness (350-500 Ω-m) lay over the basement rock. The electrical resistivity of regolith varied from 30 Ω-m to 350 Ω-m attaining its maximum thickness about 32 m. The bed rock topography indicated a gentle slope towards south and sudden rise followed by slope close to the Musi River (Figure 17). The electrical resistivity of bed rock (massive granite gneiss) ranged from 600 Ω-m to 4000 Ω-m.

4.5 Aquifer hydrodynamic properties

4.5.1 Piezometric studies

In general, the groundwater flows were from the north to south of the micro-watershed, towards the river, following the general topography. The piezometric maps were significantly influenced by irrigation pumping during the pre-monsoon season (May and

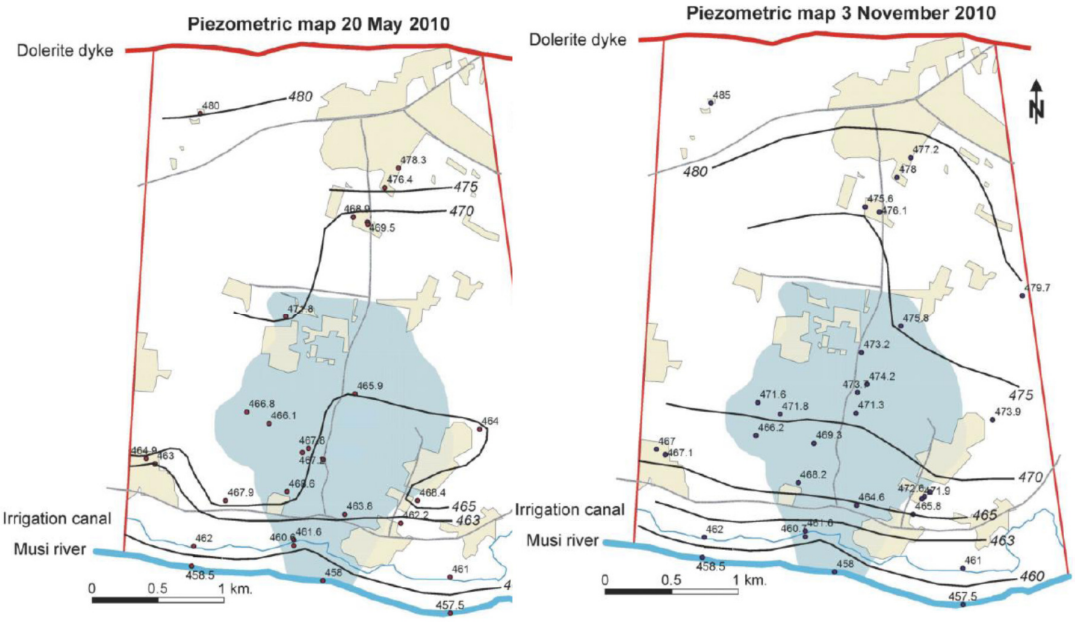

Figure 18 Piezometric maps of the micro-watershed for (a) 20/05/2010, (b) 03/11/2010. The blue area delineates the surface micro-watershed, the red lines delineate the hydrogeological catchment and light brown areas delineate built-up zones

June). During the monsoon (October and November), the pumping influence was reduced and a rise in the water table (of about 5 metres) was observed in the central part of the study area (Figures 18 and 19).

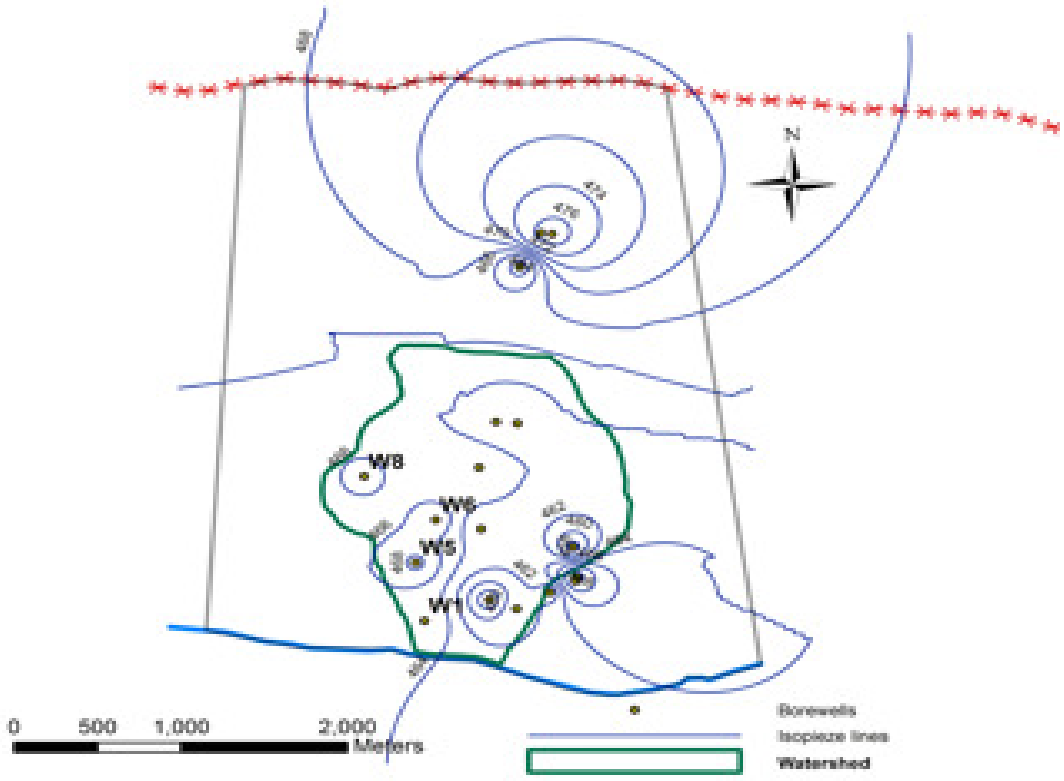

Figure 19 Piezometric maps of the study area during the post monsoon period (20/09/2013)

The piezometric levels were highly variable in both time and space under the influence of the strong heterogeneities of the aquifer and the irrigation activities. Significant variations in the water table were captured daily, and even hourly, due to the irrigation pumping activities (Figure 20). Piezometric levels in W1 and W5, which were close to the canal water, did not vary significantly during the year and were within 2 m below the ground surface (Figure 20). The water levels in this southern zone were influenced by the river which was also the boundary of the aquifer. On the contrary, piezometric levels in W8 and W6 were strongly influenced by the monsoon recharge that occurred after June as expected, in these unconfined crystalline aquifers with vertical recharge (Figure 20).

The rapid rise of the water level after each rainfall event indicated the presence of rapid preferential flow paths in the saprolite due to the existence of preserved fractures (rise of groundwater levels less than one day after rainfall event). After the monsoon, the stabilised water level was fairly constant in time (dependant of natural flow and pumping) and between the years in these two borewells.

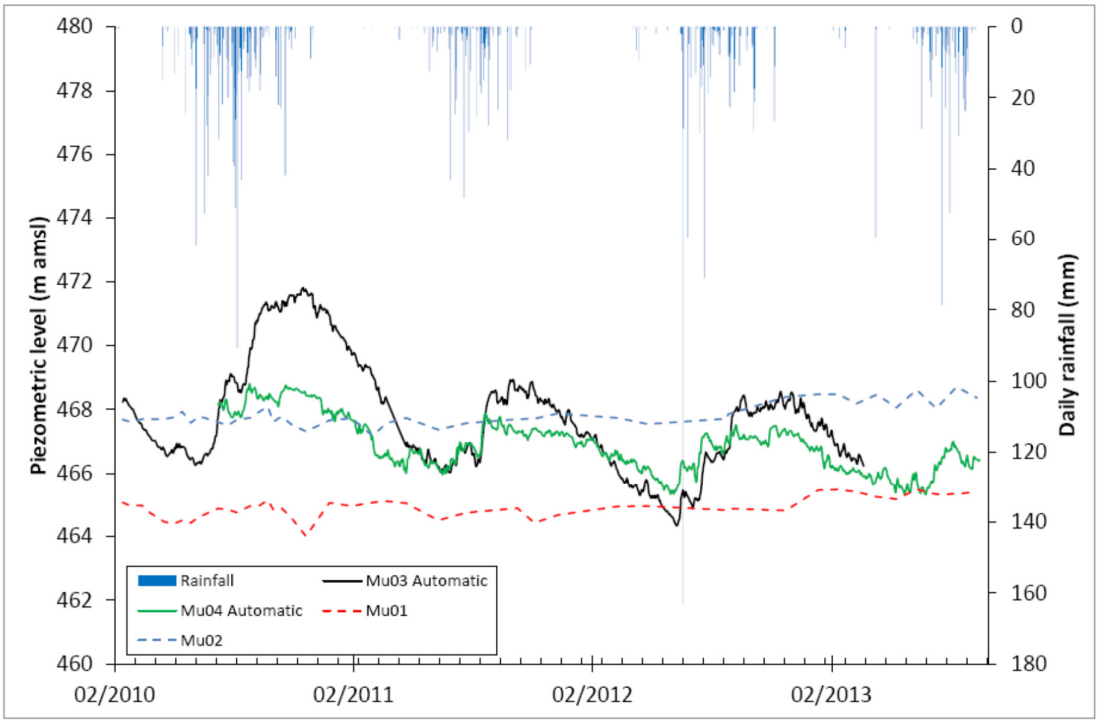

Figure 20 Water level evolution in bore wells MU01=W1, MU02 =W5, MU03 = W8 and MU04 = W6

Inter-annual piezometric levels were compared between the post-monsoon periods of 2010 and 2013. Two different zones were delineated based on the water levels; one towards the southern region of the micro-watershed where the wastewater irrigation was common. The other towards the northern end with a typical continuous decreasing water level due to over exploitation of groundwater. This was further elaborated using the Spatial Analyst module of arcview10 (IDW method), to visualise the hydrodynamic behaviour. Two distinct zones created can be clearly seen in Figure 21.

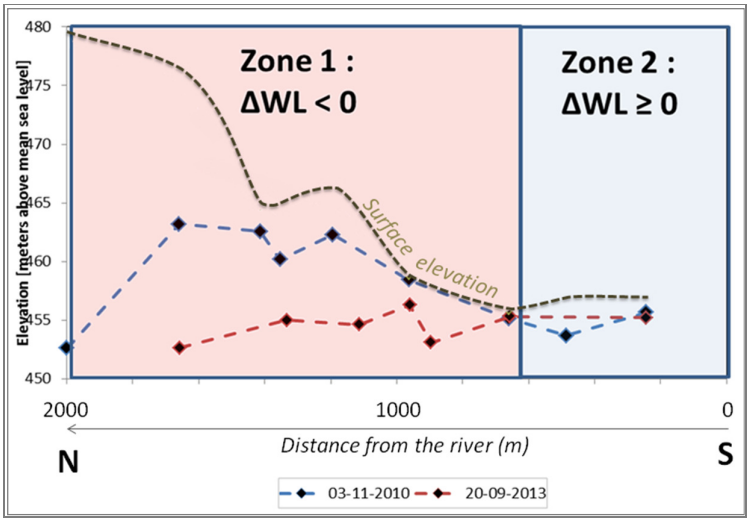

Figure 21 Water table comparison between 03-11-2010 and 20-09-2013 in the micro-watershed.

The borewells may induce constraints on water flows and impact the water table. After the monsoon due to high water levels (water table in the saprolite), the general flow was oriented in the North to South direction and one can expect the contaminant transport to occur in the direction of the river. However, during the dry season, water table levels in the northern parts declined and the tendency for the gradient of flows to be reversed was high. In this situation, the river discharge may occur towards the aquifer in the northern direction. Since the river is mostly wastewater and this action can contaminate the aquifer. Moreover, since the water table was highly influenced by the irrigation pumping, it led to heterogeneous flows creating a patchy distribution (Figure 22), which can be expected of such aquifers where the water levels fluctuate in a uncontrolled manner.

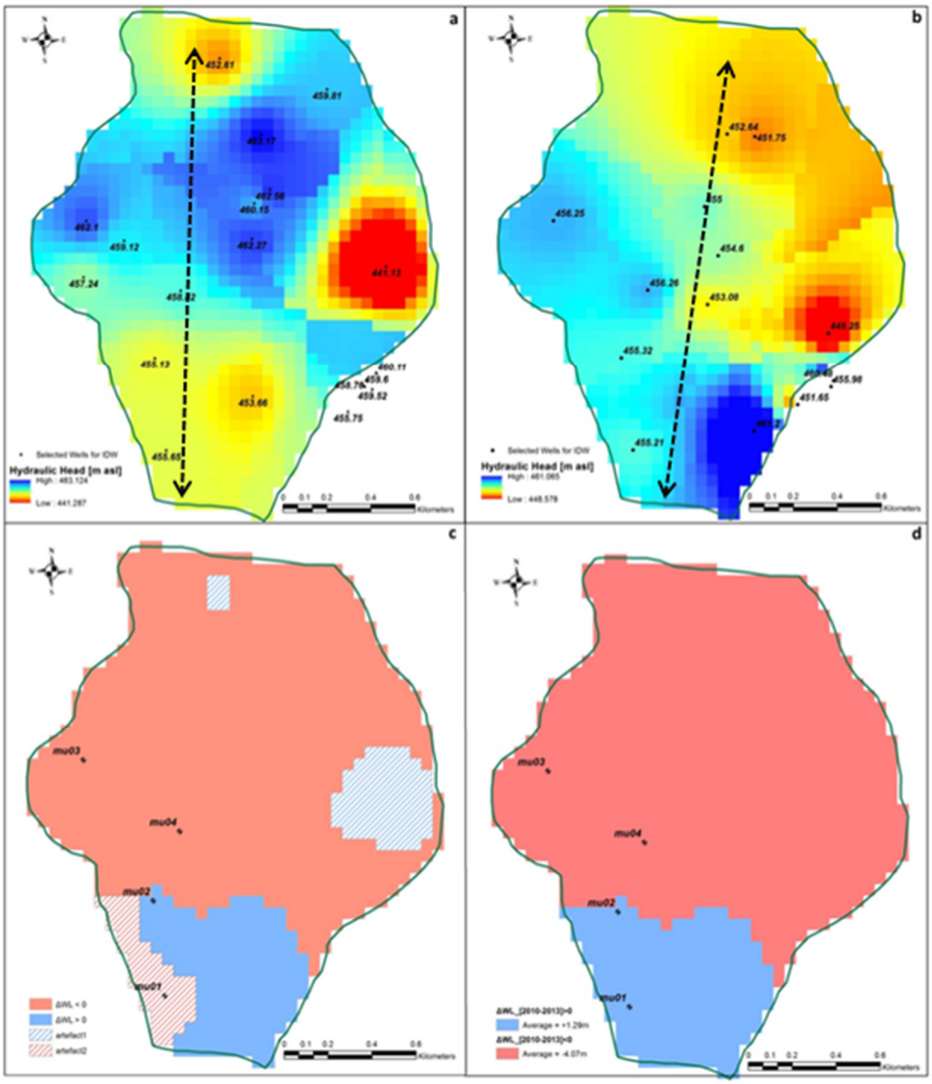

Figure 22 Computed inter-annual comparisons of the spatialized groundwater table grid. a) IDW on 03-11-2010 ; b) IDW on 20-09-2013 ; c) Water table fluctuation between 2010 & 2013 ; d) Water table fluctuation modified between 2010 & 2013

4.5.2 Pumping tests

Pumping tests were conducted at the piezometers W1, W5, W8 and W6. Each piezometer was successively pumped and observations recorded at the other piezometers on each

occasion. Drawdown was monitored during the entire pumping duration (recorded at 1-min interval). Secondly, pumping was stopped and the recovery time was recorded every minute to see how it took to reach the initial water level (Table 3). These data were used to estimate hydrodynamic characteristics of the aquifer using the software winisape developed by BRGM. The Theis method was used for interpretation with a best-fitting procedure. The results are presented in tables 4 and 5 (NB: The transmissivity of W6 was too low for an adequate pumping test to be carried out). The permeability values were in the range of the expected permeability on this geological media which usually is between 1×10^{-7} m.s^{-1} to 3×10^{-5}m.s^{-1} (Dewandel et al., 2006)

Table 4 Pumping and recovery times

Piezometer	Pumping duration (min)	Recovery duration (min)
W1	80	42
W5	55	20
W8	81	16
W6	81	29

Table 5 Aquifer characteristics

Piezometer	Discharge [l.s^{-1}]	EC (µs/cm)	T [m^2.s^{-1}]	Max drawdown [m]	K [m.s^{-1}]	S [-]
W1	0.63	1.4 -1.55	9.9 10^{-4}	0.78	1.7 10^{-5}	3.02 10^{-4}
W5	0.61	1.55 – 1.63	1.1 10^{-3}	0.59	3.4 10^{-5}	3.03 10^{-4}
W8	0.55	0.95 – 1.15	3.4 10^{-3}	0.32	7.4 10^{-5}	8.9 10^{-8}
W6	0.18	1.65 – 1.7	-	2.35	-	-

EC: Electrical Conductivity, T: Transmissivity, K: Hydraulic conductivity (K=T/e, with e, aquifer thickness). Storativity values are indicative as tests that were carried out in pumping wells (i.e., no observation wells) and during a short period.

4.5.3 Flow meter measurements

Flow meter measurements on four piezometers (W1, W5, W8 and W6) were used to describe the productive zones. According to geological logs it was possible to correlate some results with observations of cuttings. The following productive zones were identified:

- W1: productive fissure zone between 7- 8 m bgs (below ground surface) (at the top of the screen)
- W5: productive fissure zone between 10-12.5 m bgs.
- W8: productive fissure zones between 17- 17.5 m bgs, 19- 19.5 m bgs and 20.5-23 m bgs.
- W6: productive fissure zone between 12-13 m bgs.

The measurements revleaed that the flow was occurring in zones of limited extension

NB: Because of the quite low sensitivity of the flow-meter employed (25 L/min being the lowest detectable vertical flow) and the modest pumping rates, only the most productive

fissure zones have been detected. Possible secondary fracture, of minor influence may exist.

4.6 Water quality

Water resources used in the micro-watershed were a mixture of groundwater and surface water, where the latter was from irrigation canals that carried wastewater. One of the objectives of the investigations was to understand the long-term impacts of wastewater irrigation on the groundwater and the treatment capacity of the soils (SAT potential). The general groundwater flow in the micro-watershed was from north to south direction and aquifer discharge zones were apparent along the river.

Previous studies have shown that salinity and conductivity (EC) generally increased downstream of Musi River (Biggs & Jiang, 2009; McCartney et al., 2008; Amerasinghe et al., 2009). The Total Dissolved Solids (TDS) of Musi River varied over time and showing a decrease during the monsoon, probably due to a combined effect of dilution from rainfall and runoff water (Figure 23). The Musi river water had high concentrations of HCO_3^-, Cl^- Na^+ and SO_4^{2-} ions (Figure 24). Piper diagram showed significant enrichments in Na^+ in the Musi River and Cl^- and NO_3^- in groundwater and an excess of Mg^{2+} for some samples of groundwater (Figure 25).

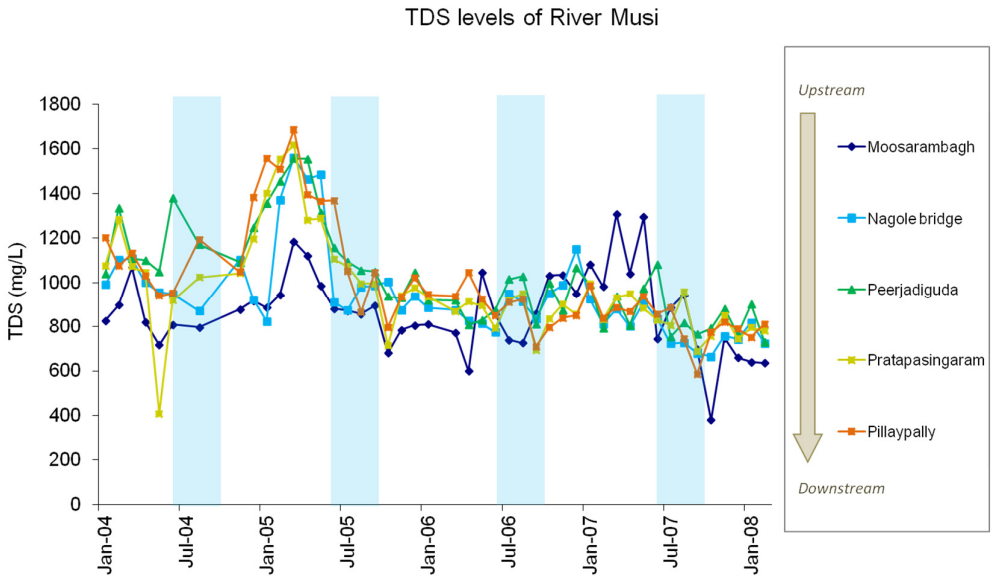

Figure 23 Total Dissolved Solids –TDS- (mg/L) from 2004 to 2008 measured at 5 stations in the Musi River (Monsoon periods are represented by blue columns). Source: APPCB

4.6.1 Surface water quality

Pre-monsoon and post-monsoon water samples collected from the micro-watershed (canal water = W2, W3 and wetland = W10, 2012) were compared with studies carried out in the same watershed in 2010, and Musi River (source water) in 2006-2008.

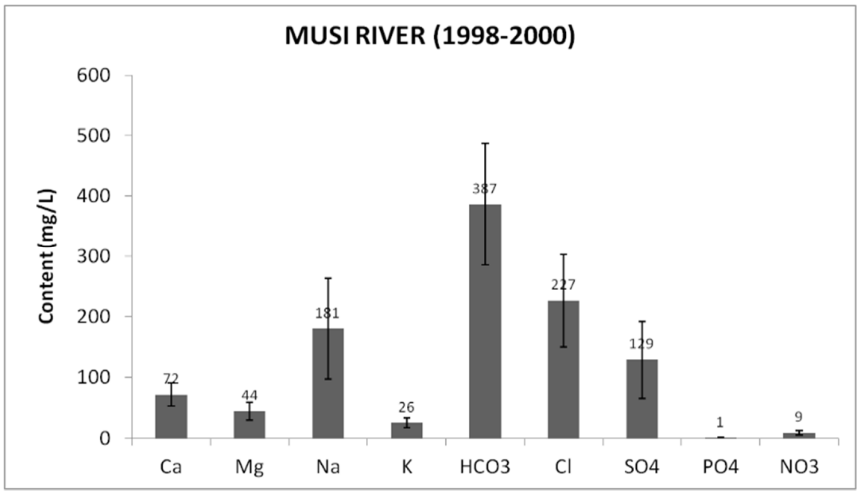

Figure 24 Mean concentrations of major ions (mg/L) of the Musi River samples collected at 5 locations from 1998 to 2000. Source: APPCB

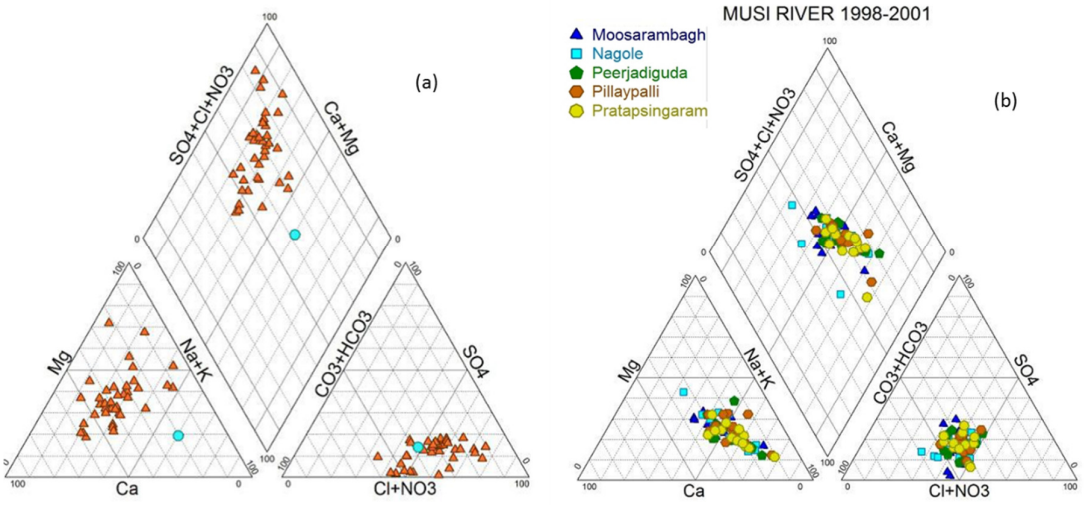

Figure 25 a) Piper diagram showing sampled groundwater near the Musi river (orange triangles) And the average chemistry of the Musi river (blue dot) in 1997 and 1998. B) Piper diagram of Musi River water collected at 4 locations between 1998 and 2001. Sources: APPCB (Andhra Pradesh Pollution Control Board) and SGWD (State Ground Water Department)

The pH ranged from 7 to 8.37 in the samples tested, and did not vary much between the pre and post monsoon samples. The electrical conductivity in the canal on the other hand, showed an increasing trend though not significant (1217 – 1490 µs/cm). This was contrary to the general expectation that monsoon will result in the lowering of EC. In the wetland sample (W10) the EC was higher than in the canal reaching 1750 µs/cm during post monsoon period. This could be due to weathering, silicate hydrolyses processes and the hydraulic gradient, which appears to be complex in this site.

Major ions (sodium and chlorides) that contribute to salinity, did not vary significantly in the pre- and post-monsoon samples, however, values were indicative of anthropogenic influences (Figures 26 and 27). The wetland sample (W10) showed a greater variation in

its constituents compared to the canal water, where it was receiving input water from multiple directions.

The canal water samples had variable nitrate concentrations ranging from 0 to greater than 150 mg/L. The high values could be due to the influence of agricultural activities as well as the source water, which carries urban run-off (Figure 27 and 28). Nitrate content in the wetland (W10) was low (<20 mg/L) probably due to denitrification processes and high organic matter loads (reeds in the wetland) (Lofton et al., 2007). It was behaving as a natural wetland attenuating contaminants. The wetland consisted of elephant grass (tunga grass), which completely covered its surface. The inlet water flows were multi-directional however, the reduction in nitrate, sulphates and phosphate levels at the outlet point (W10) was clearly evident. Investigations are being carried out to engineer this wetland to suit the needs and the discussion with stakeholders are stated in WP 6.2.

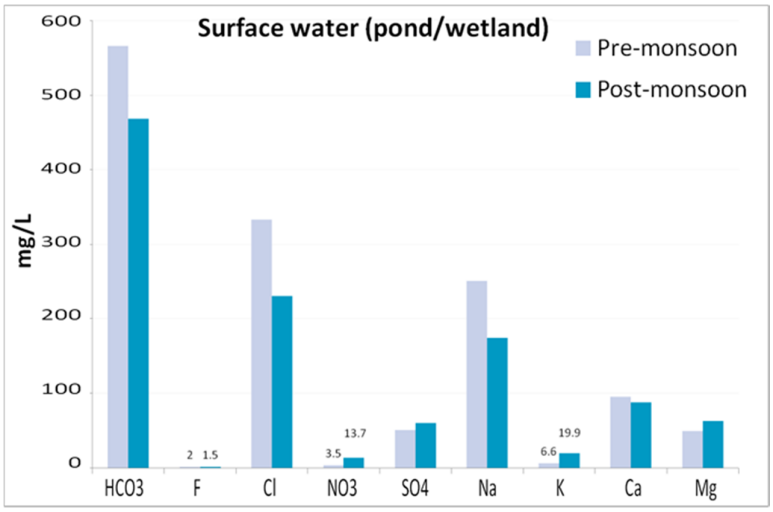

Figure 26 Pre-monsoon and post-monsoon major ion concentrations (mg/L) in the surface water samples (W10) in 2012

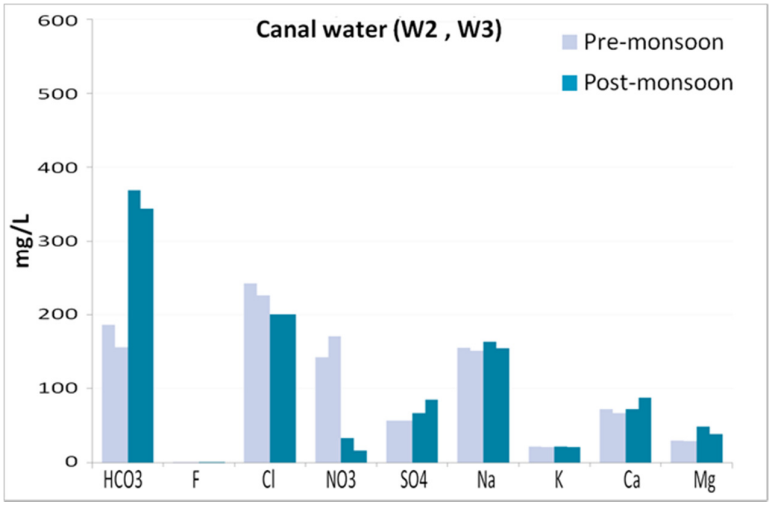

Figure 27 Pre-monsoon and post-monsoon major ions contents (mg/L) in the canal water samples (W2 and W3 sampling points) in 2012

In 2007, the Musi River BOD levels exceeded 200 mg/L in the samples close to urban areas (location A, Figure 6; Amerasinghe et al., 2009), but declined BOD values observed after 40 Km downstream (location E, Figure 6), except when some local conditions contributed to aberrant elevated levels. In comparison, for the same year, the irrigation canal at the KSMWS (15 km downstream) indicated 105 – 150 mg/L, over a period of 4 months (August to December). Apart from the biological contaminants of source water, livestock wallowing and bathing can contribute to pollution loads, as the irrigation canals are favourite places for livestock to bathe. In a more recent assessment of BOD (2013/2014), we observed that the overall values in the irrigation canal have decreased considerably, and ranged from 15-65 mg/L, probably associated with the improvements in sanitation infrastructure (STP rehabilitation and construction of new STPs) that commenced around 2009. At present, local contamination may not be contributing to these values significantly, however, the hamlet of Kachwani Singaram is expanding and will have an impact on the irrigation channels as urbanization spreads, therefore, there is a possibility that these canals may become sewage drains in the future, unless sanitation is addressed in a timely manner.

4.6.2 Groundwater quality

Water sampling campaigns in the micro-watershed carried out in 2010 and 2012 (pre and post monsoon samples) for major ions in bore wells and dug wells (11 wells out of 14 described table 1) were compared for the assessment of ground water quality. The overall profile of the major ions in all types of wells during pre and post monsoon periods are illustrated in Figure 28. The variation in concentrations for each of the major ions are described in the following paragraphs.

Electrical conductivity (EC) maps for 3 sampling campaigns in 2010 (once) and 2012 (twice) were compared. Groundwater contours along the watershed for chloride, fluoride, nitrate and sulphate for pre and post monsoon periods in 2012 are shown in Figures 31 to 33 respectively.

Results showed a strong spatial variability in groundwater chemistry (i.e. mineralisation, long term wastewater irrigation, agriculture run-off etc.). Two main poles of EC were visible: one representative of fresh groundwater with EC< 1000 µs/cm, and one pole with groundwater influenced by canal water return flows with EC>1000 µs/cm (Figure 29). It was also clear that additional sources of groundwater contamination (e.g. agriculture, sewerage) exist in the study area with localised points showing quite high EC (even higher than 2000 µs/cm). In the specific areas where groundwater was impacted by canal water return flows, the groundwater EC was higher than raw canal water most likely as a result of re-concentration by evapotranspiration processes.

Higher EC values were seen during the post monsoon period (2012) than the pre monsoon period, especially in the southern part of the watershed (Figure 30). This may be due to the increased concentrations of HCO_3^- and Ca^{2+} (Figure 28) or the strong influence of the wastewater in the canal.

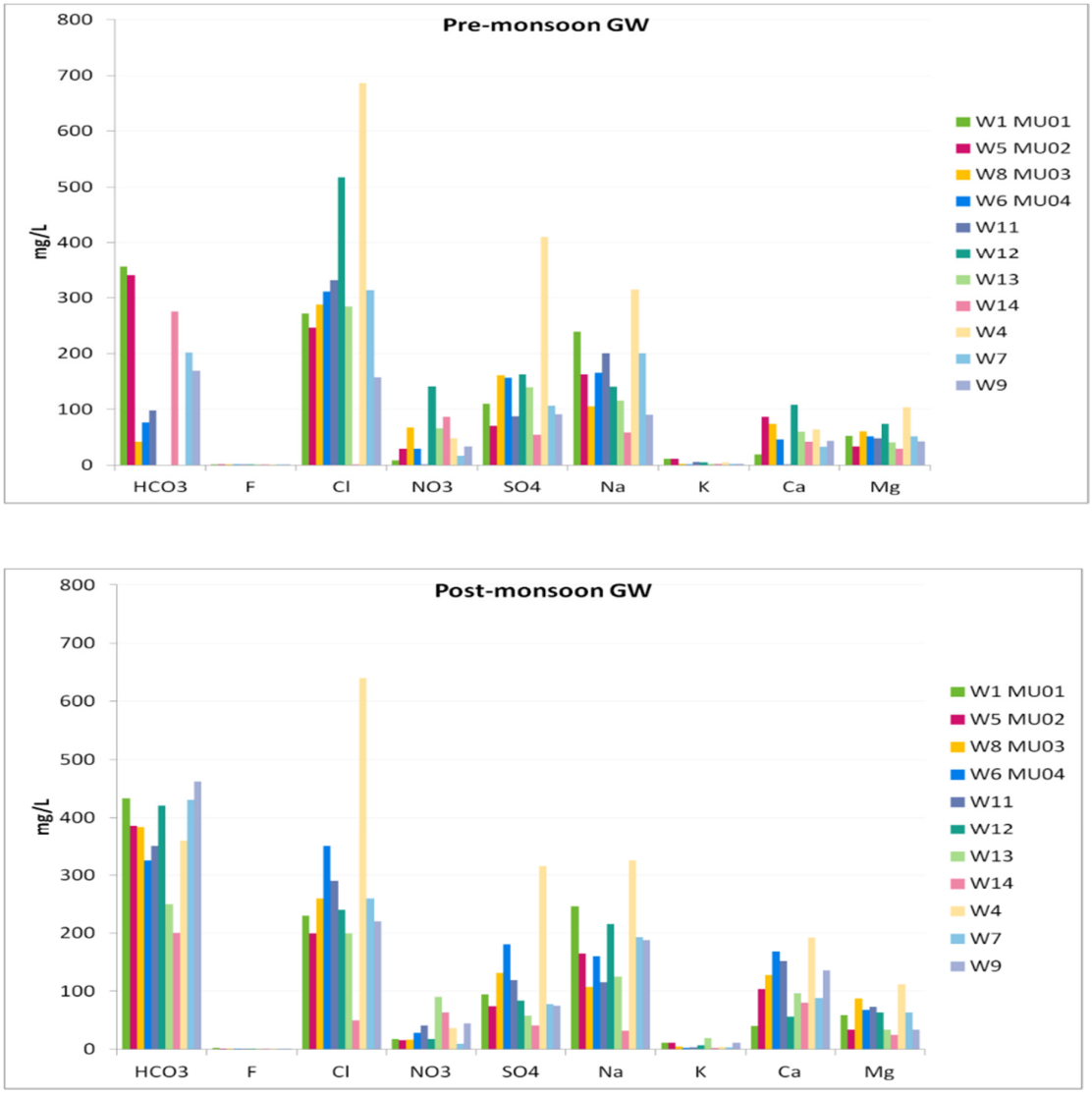

Figure 28 Distribution of major ions (mg/L) in all types of wells in the micro-watershed, during the pre and post-monsoon sampling period (2012)

A comparison of pre and post monsoon sampling showed that the chloride (Figure 31), nitrate (Figure 32) and sulphate (Figure 33) concentrations decreased under the influence of rainfall. With the exception of a slight increase in W1 well in post monsoon, there was not much variation in the fluoride concentrations in groundwater (Figure 34).

The sampled ground water shows concentration of nitrates and fluoride were above the permissible limits for drinking water (50 mg/L and 1.5 mg/L respectively, according to the WHO guidelines). Sulphate concentrations reached values up to 411 mg/L in one sample (W 4).

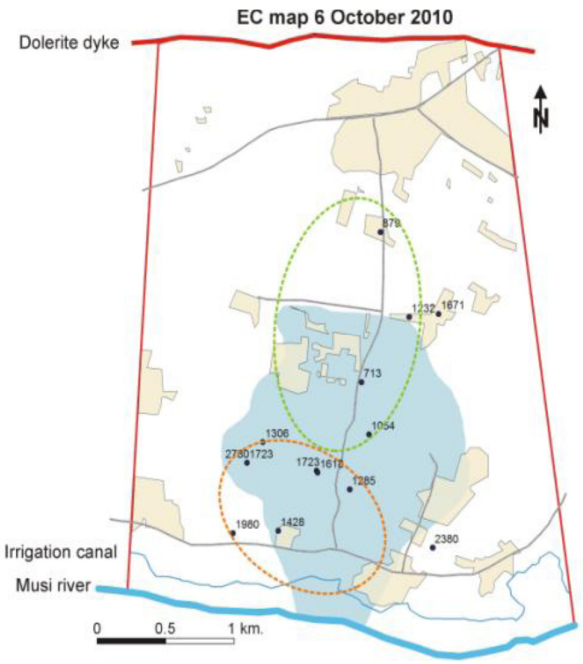

Figure 29 Groundwater electrical conductivity maps on 6/10/2010, canal water EC=1153 us/cm. The green circle outlines and area where the influence was mostly fresh groundwater (EC< 1000 µs/cm) and the orange circle delineates the area where the influence was canal water return flows (EC>1000 µs/cm) (adapted from Perrin et al., 2011)

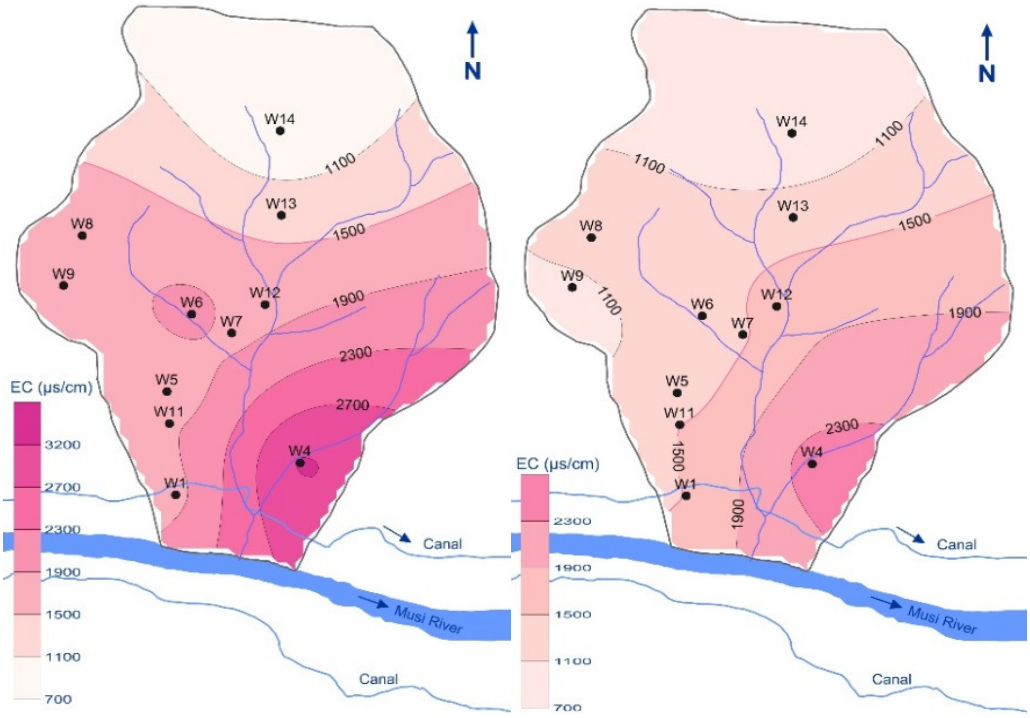

Figure 30 Electrical conductivity map pre (left) and post monsoon (right) for the 2012 groundwater campaigns in the Kachiwani Singaram micro-watershed

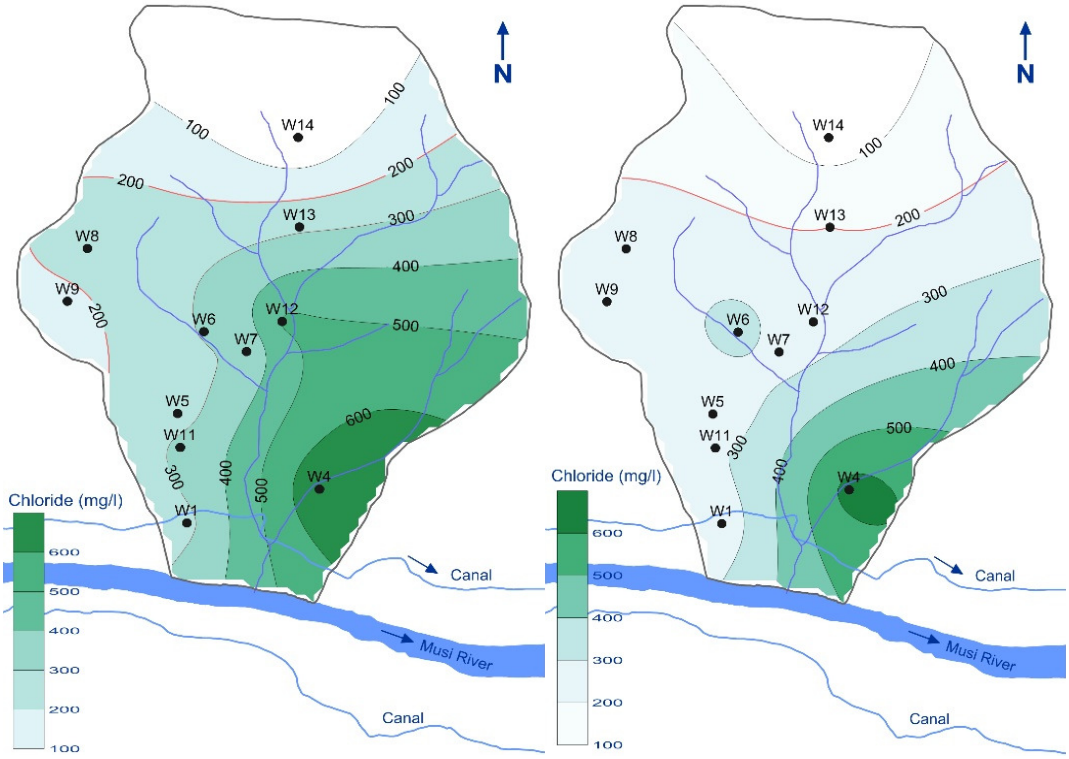

Figure 31 Chloride maps for pre (left) and post monsoon (right) for the 2012 groundwater campaigns in the micro-watershed

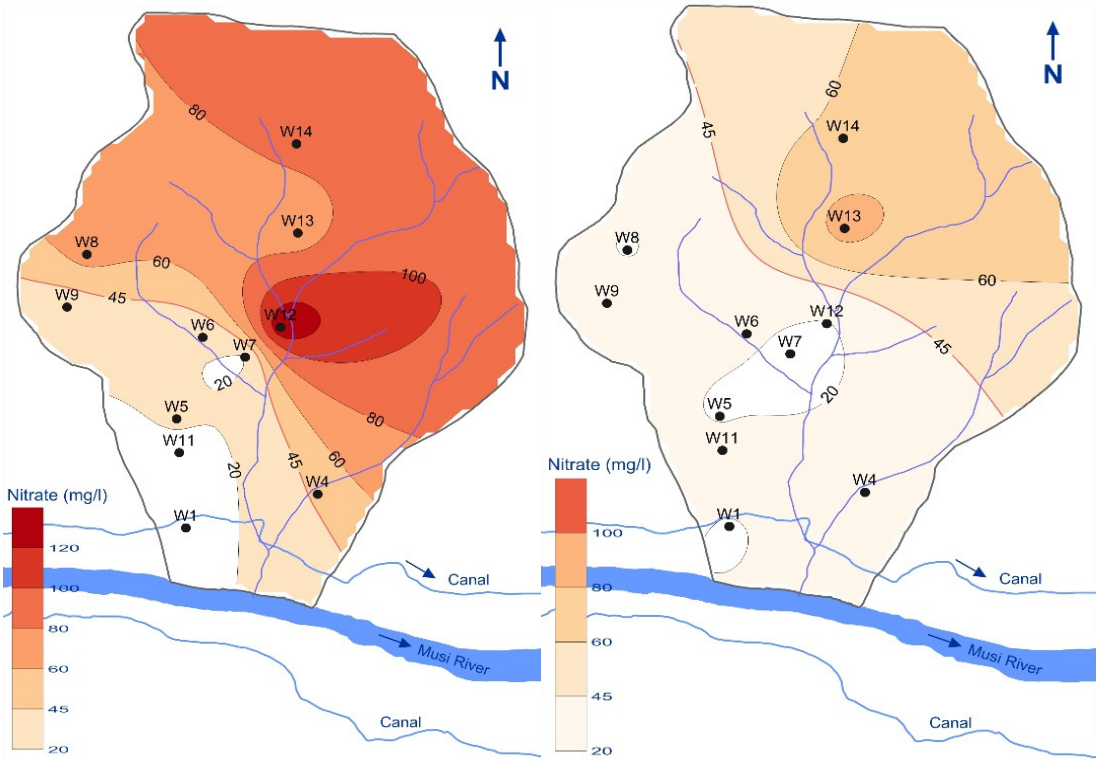

Figure 32 Nitrates maps for pre (left) and post monsoon (right) for the 2012 groundwater campaigns in the micro-watershed

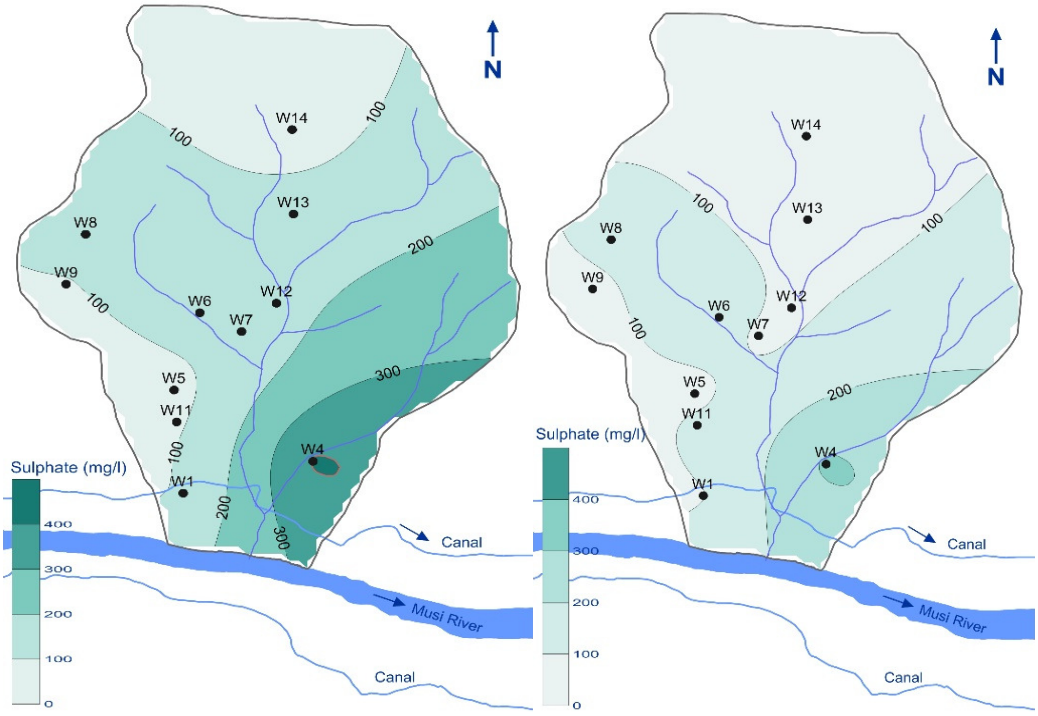

Figure 33 Sulphate maps for pre (left) and post monsoon (right) for the 2012 groundwater campaigns in the micro-watershed

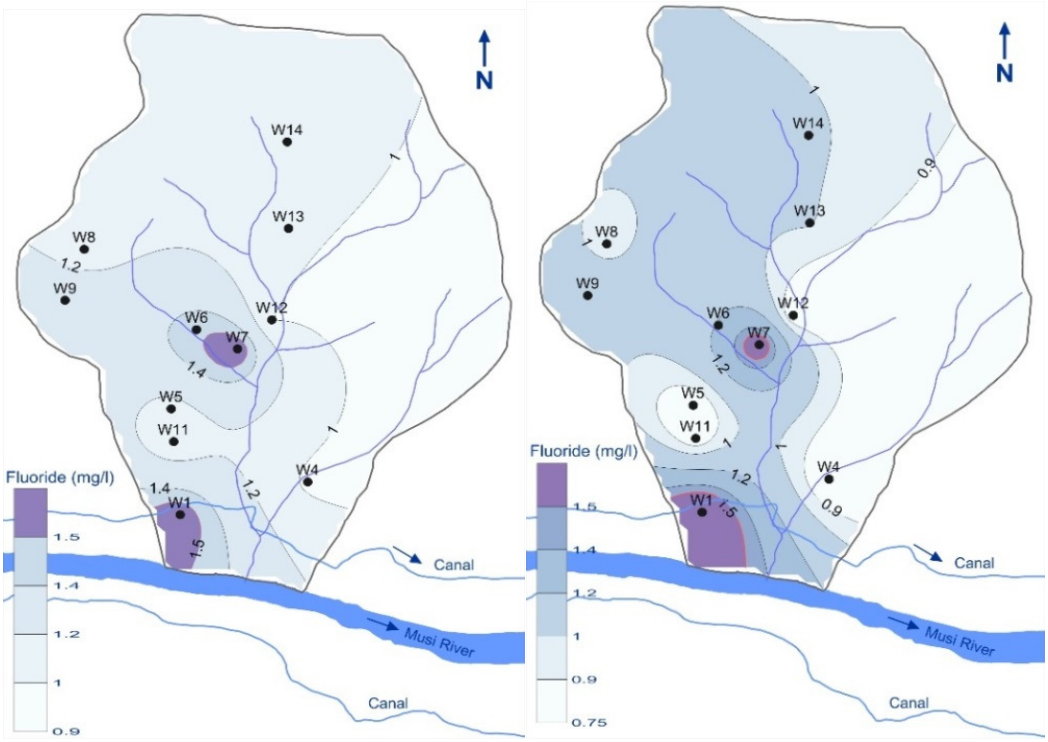

Figure 34 Fluoride maps for pre (left) and post monsoon (right) for the 2012 groundwater campaigns in the Kachiwani Singaram micro-watershed

4.6.3 Mineralization process

The analysis of groundwater chemistry with respect to each element showed that they were influenced by long term waste water irrigation, soil salinity and rainfall. High concentrations of HCO_3^- ions were due to organic matter mineralization leading to high CO_2 content in the soils. The increase in HCO_3^- content in groundwater after the monsoon could be due to the runoff processes, which results in high rates of dissolved CO_2, enhancing the mineralization processes.

The chlorides do not have lithological origin in the hard rock terrains. Therefore, it could be of anthropogenic and/or meteoric origin, enhanced by evaporation processes in soils, which decreased after the monsoon. The groundwater samples in the southern part of the catchment (W1 and W5) showed a Na^+ excess, and highlighted strong cationic exchanges within the clay minerals in the soil.

Fluoride concentrations were high and were attributed to water rock interactions enhanced by irrigation return flows (Pettenati et al., 2013). The high nitrates and sulphates were attributed to the agricultural practices and wastewater irrigation impact on groundwater.

Chemical water facies were classified using piper diagrams (Figure 35). It showed that temporal variations of major ions due to rainfall were not significant, and anthropogenic activities like wastewater irrigation, application of fertiliser, soil salinity may be contributory to the increased levels of nitrates and sulphates.

Groundwater samples from piezometers (W1, W5, W8 and W6), that were used only for monitoring purposes illustrated the spatial and temporal variability (2010 and 2012) of water quality within the micro catchment:

- W1=MU01: variability in the chemical facies was not that significant in the monitoring years 2010 and 2012, and was not influenced by the hydrological condition that prevailed. However, of the ions that were considered important for irrigation, sodium, chloride and TDS were at moderate restriction levels.
- W5=MU02: a strong spatial variability at different depths was observed for EC during 2010. In general, influence of the monsoon period can be regarded as minimal 2012.
- W8=MU03: variability in EC was observable in 2010, however, no clear trend can be attributed. Effect of the monsoon was minimal in 2012.
- W6=MU04: variability in the water quality facies indicate that monsoon had little impact.

A comparison of the sodium/chloride scatter plots showed that there was high temporal variability during the 1998-2000 period in the river water. A comparison with groundwater samples for 2012 did not show much variability, although marginal shifts were noted. Most fall along the equi-potential line as seen in the Figure 36.

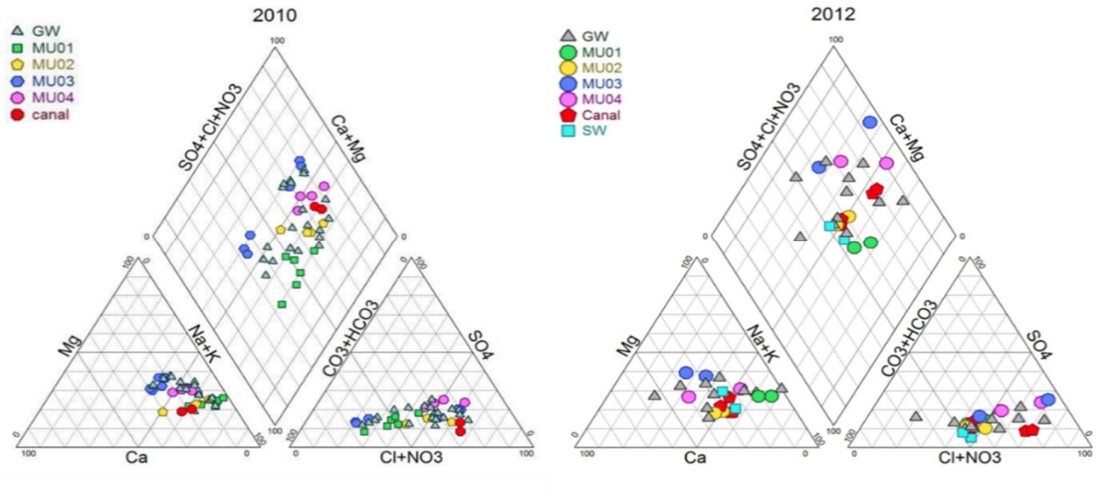

Figure 35 Piper diagram of groundwater samples and irrigation canal water collected in the micro catchment in 2010 and 2012. W1=MU01, W5=MU02, W8=MU03 and W6= MU04 are the scientific bore wells dug in 2009 and GW spots represent farm bore and dug wells

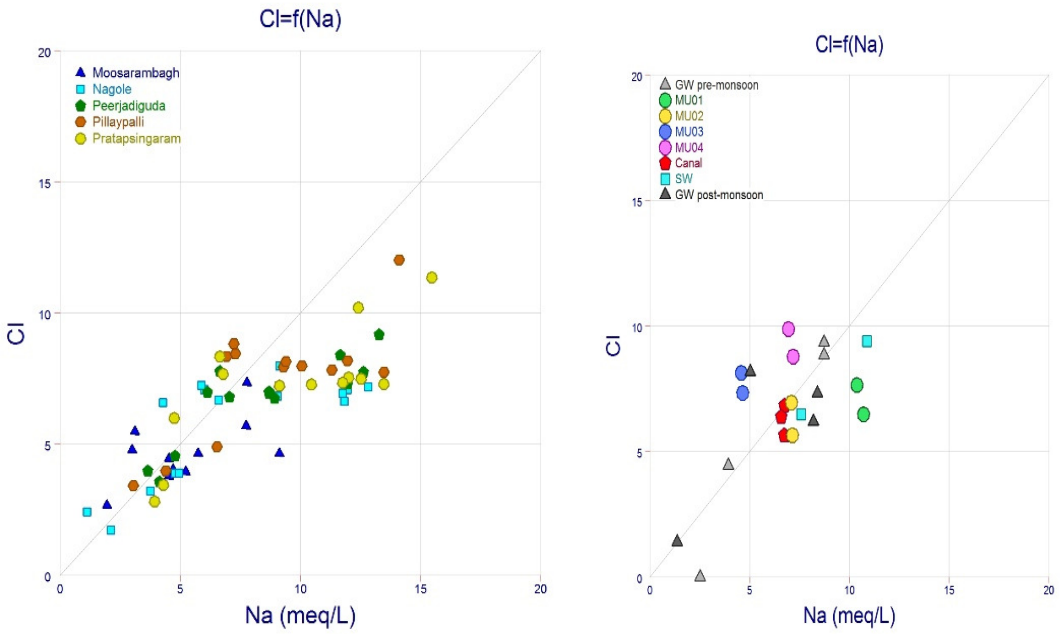

Figure 36 Chlorides vs Sodium scatter plot for Musi River (1998-2000) APPCB data (a) and groundwater samples in 2012 (b) Mooserambagh to Prathapsingaram is around 20 km stretch covering a large portion of the city. W1=MU01, W5=MU02, W8=MU03, W6=MU04 (piezometers); GW = agriculture bore wells (n=4)

The influence of wastewater irrigation on the wells W1, W5 and W8 were obvious in relation to sodium and chloride concentrations, and is most likely were associated with the agricultural activities in the locality. The W6 did not appear to be impacted by the wastewater irrigation practices, which was interesting. In general, for the micro-watershed one can say that wastewater irrigation coupled with clay mineralization would have contributed to the sodium excess. Excessive irrigation return flows, through solute recycling would have led to the significant aquifer salinization further exacerbated by the

presence of thick clay soils (geophysical study), which favoured strong cationic exchanges (Perrin et al., 2011).

4.6.4 Electrical conductivity (EC) logging

In each piezometer, electrical conductivity logging was carried out on three occasions (January, July, and November 2010). Measured EC was corrected for temperature (Figure 37). In W1, a progressive increase in EC was observed; higher values in the top part were only observed in January; it was noted that EC values in groundwater were systematically higher than EC values of canal water. This difference was attributed to further enrichment caused by evaporative and leaching processes.

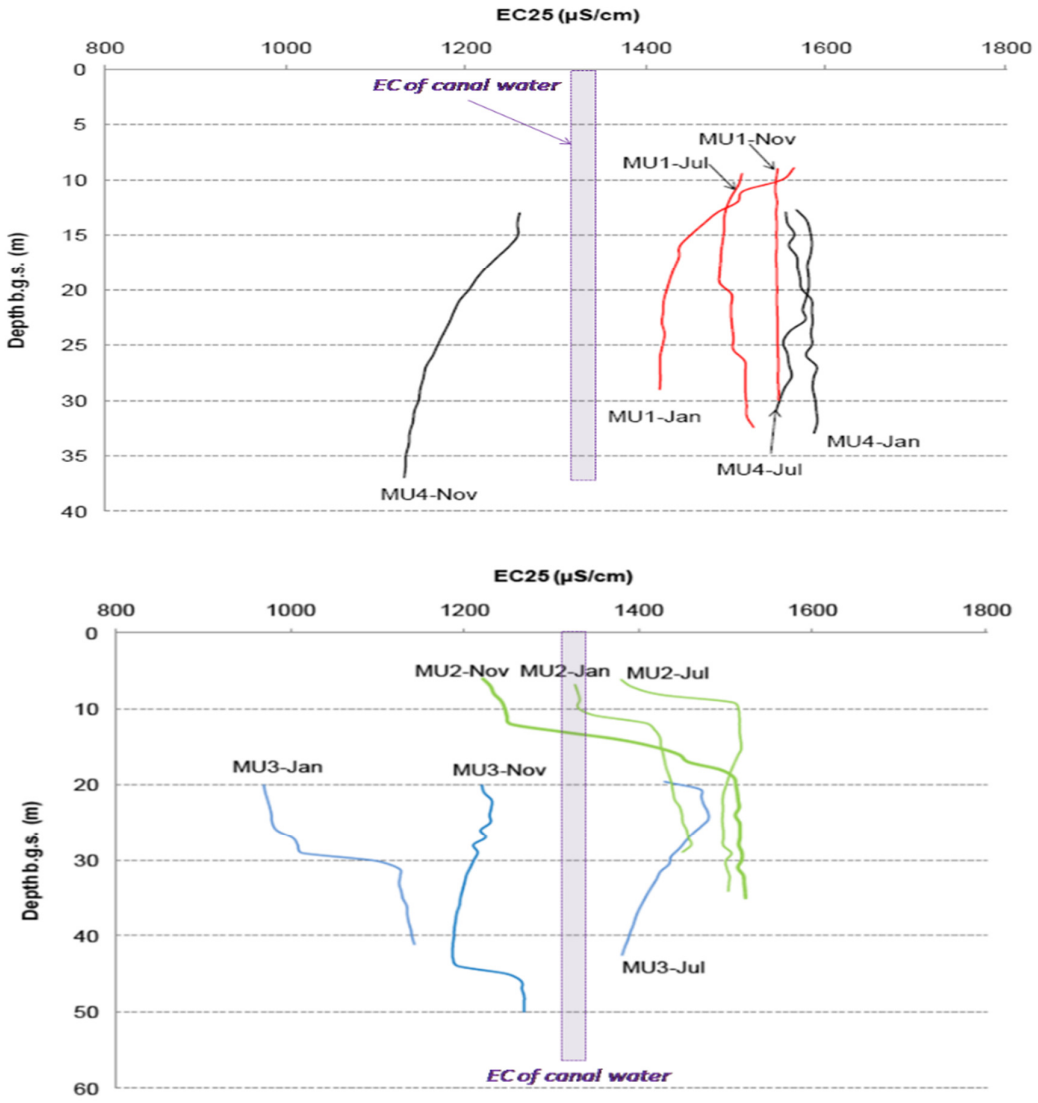

Figure 37 Electrical conductivity logs (EC) of piezometers a) W1 and W8 (MU01 and MU04) b) W5 and W8 (MU02-MU03); three successive measurement campaigns are presented (26 January, 09 July, 24-25 November 2010). Only data measured below the plain casing are reported. For comparison canal EC was 1332, 1335, 1316 µs/cm for 26 January, 09 July, 25 November 2010 respectively.

In W5, EC above 10 m bgs (below ground surface) (i.e., in the saprolite) was close to values measured in canal water with additional dilution noted in November, which was attributed to monsoon recharge. Below 10 m, EC values were in the same range (around 1450 µs/cm) also similar to values observed in W1. The lower values observed in the saprolite may have been due to the fact that the piezometer was located within a wastewater irrigated area, and reflected the canal water chemistry. Compared to all the wells, W6 (November, 2010) and W1 (January,2010), displayed dilution effects, although the reasons for the two could be different. The W6 was most definitely linked to the monsoon recharge, whereas the W1 may have been influenced by continuous flooding that took place in the locality for rice irrigation.

The EC logs of W8 exhibited a high temporal and vertical variability with lower values in January and November 2010, and higher values in July similar to W1. It is possible that in July, low piezometric heads in W8 caused temporary inversion of the hydraulic gradient (Figure 37). On the contrary, in January and November, when groundwater abstraction was high, and higher peizometric heads were observed, the weathering processes were less than during the monsoon period, and the trend showed little variation. Abrupt EC changes at around 30 m and 44 m bgs suggests the presence of active flow fractures.

4.6.5 Suitability for irrigation

The cations and anions contribute to the overall EC and will determine the suitability of the water for irrigation purposes. The high EC observed in the study area could be due to ions of anthropogenic origin which in this setting was mostly agricultural activities as well as the city water that is used for irrigation. The studies of 2007 showed that EC levels increased, and more particularly the chlorides, where the values reported were higher than 10 meq/L (350 mg/L), and SAR (sodium adsorption ratio) greater than 9.

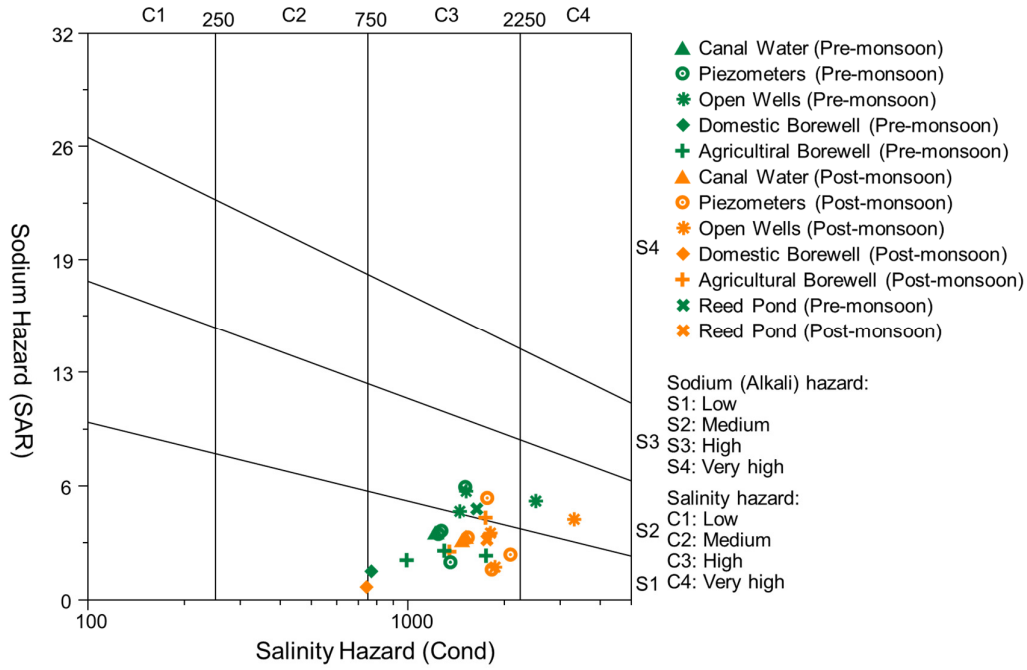

Figure 38 Water quality for irrigation suitability (Wilcox Diagram) (pre-monsoon and post-monsoon data of 2012) in the micro-watershed

Within the micro-watershed, the Wilcox diagram for salinity hazard vs sodium hazard fell under C3S1, C3S2 and C4S2 categories, which indicated a high salinity hazard (Figure 38) and therefore, not suitable for sustainable irrigation. Farmers also stated that many have had to abandon paddy cultivation and switched to paragrass (*Urochloa mutica*) cultivation which is saline tolerant. The study showed that long term wastewater irrigation has impacted the local groundwater quality, and the local inhabitants have confirmed that the water has become more saline over the years.

4.6.6 Distribution of pesticides in water samples

Of the 14 samples tested, only 7 (W1, W2, W3, W5, W7, W10 and W14) showed the presence of pesticides, at levels that were detectable. They belonged to three families, namely, organochlorine, organophophorus and carbamate. Farmers in the study area were using organochlorine pesticides (OCP's) like butachlor, organophosphorous pesticides like (OPP's) like malathion and carbamate pesticides like carbofloro nuclon granules.

The pre and post monsoon sampling campaign results showed a high temporal variability in the pesticide concentrations in groundwater (0.01 – 0.09 µg/L). W14 had the highest number of pesticide residues in the pre-monsoon period, which was not detected during the post-monsoon sampling. A single domestic bore well tested positive and there was a paucity of the information on pesticide used by people in this locality.

In general, one can expect the monsoon rains to dilute pesticide concentrations, but there were instances where elevated levels were observed ever after the monsoon, which was attributed to leaching and agriculture runoff (canal water (W2) samples). Some pesticides like propoxure were not in use, but were found in W5, and canal samples (W2 and W3). This requires further investigations that involves neighbourhoods. Another pesticide, Atrazine that was not used by the farmers was also found in some of the wells, and further studies are required to see the origin of these pesticides.

The presence of pesticides in the canal water can be due to many sources other than the agriculture runoff, as some of the pesticides recommended for agriculture purposes are used for domestic pest control as well. However, studies on other sources were beyond the scope of this study. The permissible limit for drinking water as per BIS (Bureau of Indian Standards) standards for each pesticide is 0.01 µg/L, and most samples showed values higher than 0.01 µg/L. Even though people were not drinking the water either from the canal or local groundwater wells that were tested, the elevated concentrations of pesticide elements raise a question on the impact on the environment and biodiversity and possible accumulation in the food chain.

4.7 Groundwater budgeting

The groundwater budget of the watershed was expressed as given in Perrin et al., 2011 (For example, during a hydrological year, the groundwater Inflow (Inputs) equals the groundwater outflow plus or minus the change in Groundwater Storage):

$R + Rf + Qin \pm Lc - P - E = Qout$

Where R is the natural recharge during the monsoon, Rf is the return flows (mainly from wastewater/groundwater irrigation but also from domestic water uses), Lc, is canal losses

or gains, Qin is groundwater inflow across groundwater reservoir limits, P, groundwater pumping, E, evaporative discharge from the water table, Qout the groundwater contribution to Musi river base flow.

The simplified steady state budget at the micro-watershed scale was calculated using the average values of recharge and pumping and by neglecting the change in groundwater storage, and losses or gains of the canal (Maréchal et al., 2006). As there was no significant groundwater inflow across groundwater reservoir limits it was assumed as 0 mm/yr. The average annual rainfall at the study watershed was 740 mm/yr and estimated recharge calculated from monitored groundwater level data at the irrigated sites of the study area was 81 mm/yr, but by considering the non-irrigated parts of the watershed (built-up, fallow land) (23% of the total area), the total groundwater recharge from rainfall estimated by Perrin et al. 2011 was only 70 mm/yr.

Table 6 Irrigated areas of the study area with different sources of water and corresponding irrigation amount and coefficient of return flows (Modified from Perrin et al. 2011).

Source of water	Crop	Irrigated area (ha)	Irrigation (mm/d)
Ground water	Paddy	12.9	15.0
	Vegetables	0.58	9.5
	Fruits	0.35	9.5
Mixed	Paddy	2.86	15.0
	Paragrass	7.2	11.0
Canal	Paddy	22.9	15.0
	Vegetables	7.0	9.5
	Paragrass	106.2	11.5

NB: mixed irrigation water is assumed to be half groundwater and half canal water.

Evaporation from the shallow water table was estimated using the Coudrain-Ribstein equation depending on depth of the water table (Coudrain-Ribstein et al. 1998). The total estimated evaporation losses from the aquifer were approximately 7 mm/yr. Groundwater pumping estimated from discharge on 26 borewells was estimated at 70 mm/yr in the area (Perrin et al. 2011). Approximately 65 mm/yr were used for irrigation and 5 mm/yr for domestic use. Irrigation volumes from wastewater extraction were estimated from water extraction measurements from the canal. Taking into account the irrigation source, the corresponding area and return flow coefficient defined by Dewandel et al. (2008) for the different crop types (Table 6), irrigation return flow was estimated at 143 mm/yr. 70% of the irrigation return flow was from waste water irrigation (113 mm/yr) and 30% was from groundwater extraction (29 mm/yr) and a small part of the return flow at the watershed scale (0.9 mm/yr) was from domestic water recharges (Perrin et al., 2011). The study showed that the wastewater irrigated systems in the study area contributed significantly to the irrigation return flows. The estimated groundwater outflow from the watershed or groundwater contribution towards Musi river base flow was 136 mm/yr, groundwater

contribution towards the Musi River was 0.4% of the river flow. The studies over the years have shown that wastewater irrigation has contributed to the base flows of the Musi River.

5 Synthesis: Conceptual model

The peri-urban micro-watershed comprised a number of land uses and the dominant types were agriculture, buildings, barren land, and a small natural wetland with reeds. The hydrodynamic monitoring, hydraulic test, hydro-geophysical surveying, land use data, and water chemistry data were utilized to develop the conceptual model for flow and transport (Figure 39). The lithological conceptualization is depicted in Figure 40.

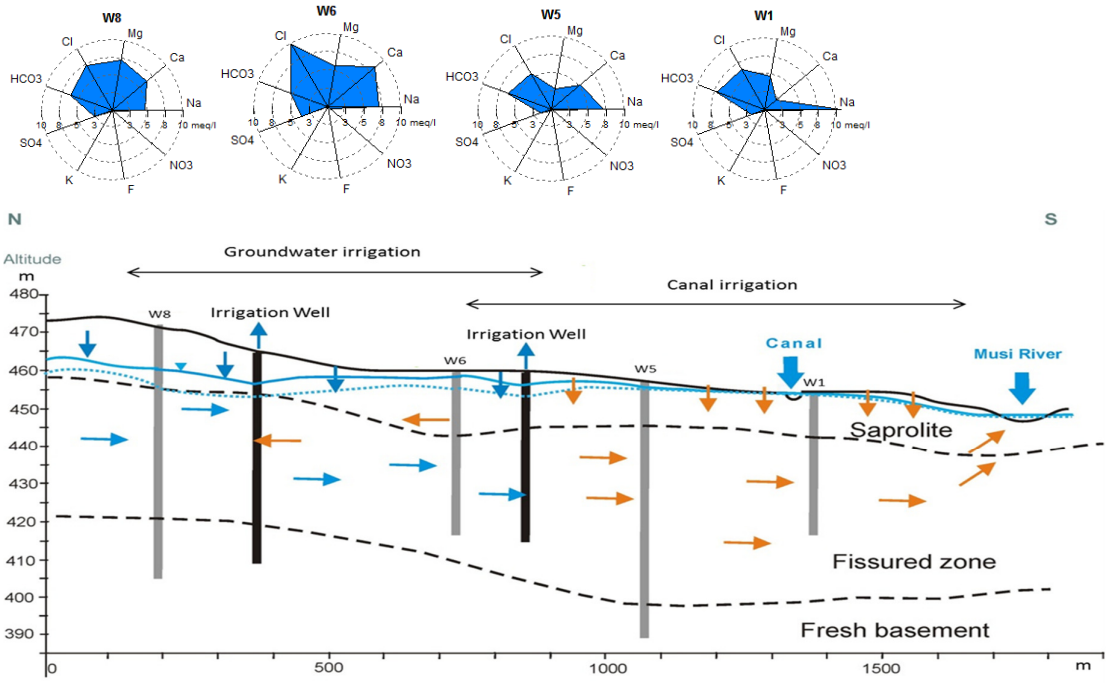

Figure 39 Conceptual model of groundwater flow and transport. W8, W6, W5 and W1 are piezometric wells. The irrigation wells are used for agriculture. The water chemistry radial plots, corresponding to 4 piezometers and one canal (W2) samples are illustrated. (adapted from Perrin et al 2011). Dotted blue line – pre-monsoon (June); Blue line – post monsoon (November)

The water budget showed that the canal irrigation was the main recharge flux at the basin scale and had a strong impact on groundwater quality. In such hard rock aquifers, the saprolite plays a storage role due to its porosity, and the fissured zone provides the transmissive function. When the water levels are high, the saprolite layer allows a regional ground water flow. In the micro-watershed, the ground water flow was from north to south, towards the Musi River. However, when intense pumping occurs, the water levels decrease in the northern regions of the micro-watershed. The return flows then induce a mixing of the groundwater and canal water (pumped for irrigation) in the middle potion of the watershed, which ultimately contributes to groundwater recharge with mixed water. Long term wastewater irrigation in the area has resulted in high ground water salinity, and agriculture run-off may have also contributed to it (e.g. Nitrates, pesticides). The Musi River (within the micro-watershed) and W1 and W5 share similar hydrogeological conditions with minimal variations in relation to water levels. Thus, the canal plays only a passive role on the hydrogeology in the southern part of the micro-watershed.

The groundwater quality survey showed that the contaminant sources could be many (e.g. river water, agriculture run-off, local hamlet run-off, local compost industry etc.) and heterogeneous at the micro-watershed scale. In general, the northern part had more nitrate and pesticides contaminants, and were attributed to the agricultural inputs. A significant water-rock interaction was also evident, for example, elevated fluoride content in the ground water samples.

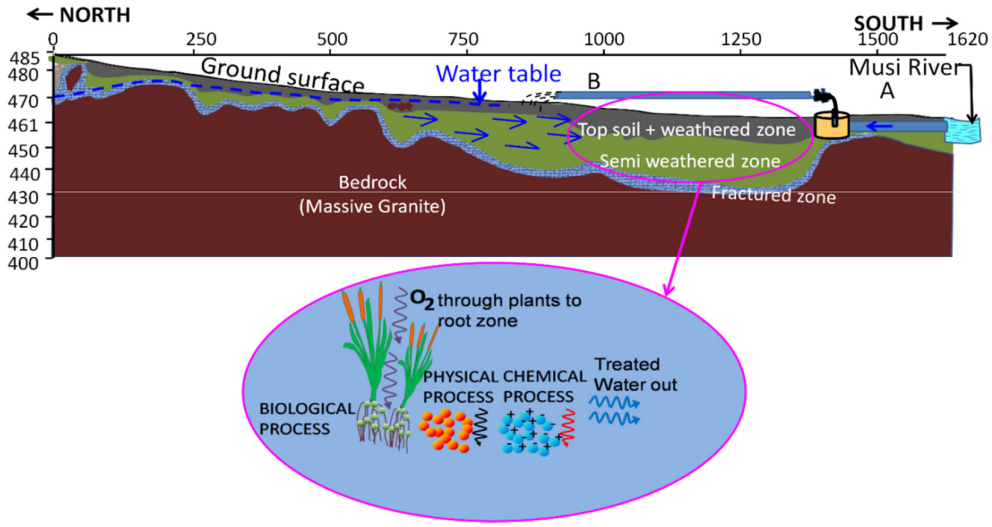

Figure 40 Lithological conceptual model of the micro-watershed

Geological conditions revealed by geo-physical studies showed that in the small wetland area, there is a deeper weathered zone, which may provide suitable conditions for wetland function. The formation of the hardrock aquifer system in the watershed is complex and therefore, the ground water flow varied from 430 - 472 m amsl.

6 Conclusions and recommendations

The study showed that the groundwater and surface water interactions are complex in this micro-watershed due to heavy groundwater abstraction and wastewater irrigation. A high degree of variability in water quality was observed due to the local level activities. The water flow pathway, which is mainly from north to south during high water level conditions, appear to suggest that SAT processes might be occurring, however, it is not a year round phenomenon, as the flow becomes directed to local depressions in the dry season. Therefore, one can expect some degree of SAT, but not to a level that is useful for irrigation purposes.

The ground water was affected by the practice of wastewater use for irrigation as seen with elevated levels of selected elements, which are commonly found in wastewater. Further, it appears that the geological formation and weathering processes also impact the groundwater quality. Some elements, did not meet the recommended standards for irrigation use.

Pollution sources in this study site were numerous and could be from:

- Agriculture (nitrates observed in the northern part of the area; pesticides),
- Water rock interactions (fluoride) enhanced by intense agricultural practices in most of the basin

- The river (city wastewater with numerous health risks)

Considering the different hydrological and geological interactions, Soil Aquifer Treatment may not be a direct solution for treatment of the wastewater, except for a few elements, in this site. The geophysical studies performed showed zones with relatively deep weathering (potentially inducing high permeability, thus facilitating contamination) but the limited size of the area, and the continuous irrigation for agricultural activities may not allow the required retention time for treatment prescribed for the soils in the area. Further, the return flows may increase mineralization and increase the fluoride release from the rocks. More studies are needed to understand the flow patterns under the geologic conditions of this micro-watershed. Thus, the interaction between irrigation water, plant uptake, soil retention, and biogeochemical reactivity should be further investigated. Past studies have shown that some soils had elevated levels of heavy metals although they were below the permissible levels (Amerasinghe et al., 2009). It is possible that this situation can worsen over time with continuous irrigation. Therefore, monitoring the water, soil and plant quality at intervals is important.

Finally, although the potential for SAT may exist in this watershed, the complex hydrogeologic conditions may not be conducive for pollutant attenuation under natural conditions. Regulation of abstraction can be recommended if a Managed Aquifer Recharge program is to be adopted. However, this is not feasible in reality as the bore wells are owned by farmers and restrictions on pumping are difficult to impose. Given the fact that the electricity supply is free (provided for 7 h/ day), controlling private bore wells may not be a viable option.

Studies on the naturally occurring wetland, offers new opportunities. It is possible to engineer such wetlands to suit the farmer needs locally. Since these farmers have not tested on-farm treatment systems, awareness raising will be an important strategy, before launching a pilot study. As such, the options for natural and engineered wetlands based on the wetland functions observed in the study site should be further explored. Further, these wetlands need not be large. Small scale units can be equally effective and could be an immediate solution to safe food production. More work needs to be done on the design aspect, as well as the treatment capacity.

7 References

Amerasinghe, P., Weckenbrock, P., Simmons, R., Acharya, S., Blummel M. 2009. An atlas of water quality, health and agronomic risks and benefits associated with “wastewater” irrigated agriculture an atlas of water quality and agronomic risk and benefits associated with "wastewater" irrigated agriculture. A study from the banks of the Musi River, India. Published online: http://www.freidok.uni-freiburg.de/volltexte/6963.

APHA 2005. American Water Works Association and Water Pollution Control Federation. Standard method for the examination of water and wastewater, (21st ed.). New York: American Public Health Association.

Ayers, R.S., Westcott, D.W. 1994. Water quality for agriculture. FAO irrigation and drainage paper 29 Rev 1. Http://www.fao.org/docrep/003/t0234e/t0234e00.htm.

Biggs, T.W., Jiang, B. 2009. Soil Salinity and Exchangeable Cations in a Wastewater Irrigated Area, India. Journal of Environmental Quality Vol 38: 887-896.

Buechler, S., Devi, G., Raschid, L. 2002. Livelihoods and wastewater irrigated agriculture: Musi river in Hyderabad city, Andhra Pradesh, India. Papers published in Journals (Open Access), 8(h032354), 14-17.

Chandra, S., Rao, V. A., Krishnamurthy, N. S., Dutta, S., Ahmed, S. 2006. Integrated studies for characterization of lineaments used to locate groundwater potential zones in a hard rock region of Karnataka, India. Hydrogeology Journal, 14(6), 1042-1051.

Chandra, S., Ahmed, S., Ram, A., Dewandel, B. 2008. Estimation of hard rock aquifers hydraulic conductivity from geoelectrical measurements: a theoretical development with field application. Journal of hydrology, 357(3), 218-227.

Coudrain-Ribstein, A., Pratx, B., Talbi, A., Jusserand, C. 1998. Is the evaporation from phreatic aquifers in arid zones independent of the soil characteristics? C.R. Acad. Sci. Paris, Sciences de la Terre et des Planètes 326: 159-165.

Dewandel, B., Lachassagne, P., Wyns, R., Maréchal, J.C., Krishnamurthy, N.S. 2006. A generalized hydrogeological conceptual model of granite aquifers controlled by single or multiphase weathering. J. Hydrol., vol. 330: 260–284.

Dewandel, B., Gandolfi, JM., de Condappa, D., Ahmed, S. 2008. An efficient methodology for estimating irrigation return flow coefficients of irrigated crops at watershed and seasonal scales, Hydrological Processes 22: 1700–1712.

Ensink, J.H.J., Blumenthal, U.J., Brooker, S. 2008. Wastewater quality and the risk of intestinal nematode infection in sewage farming families in Hyderabad, India. American Journal of Tropical Medicine and Hygiene 79(4): 561-567.

Ensink, J.H., Scott, C.A., Brooker, S., Cairncross, S., 2010. Sewage disposal in the Musi-River, India: water quality remediation through irrigation infrastructure. Irrigation and Drainage Systems. 24(1-2), 65-77.

Guihéneuf, N., Boisson, A., Bour, O., Dewandel, B., Perrin, J., Dausse, A., Viossanges, M., Chandra, S., Ahmed, S., Maréchal, J.C. 2014. Groundwater flows in weathered crystalline rocks : impact of piezometric variations and depth dependent fracture connectivity. Journal of Hydrology 511: 320-334.

Lofton, D.D., Hershey, A.E., Whalen, S.C. 2007. Evaluation of denitrification in an urban stream receiving wastewater effluent. Biogeochemistry 86: 77-90.

Mahesh, J., Amerasinghe, P., Pavelic, P. 2015. Elucidating changes in land use patterns, crop choices and farmer perceptions in a wastewater-dominated peri-urban agricultural system in India". R.S. Deshpande, Prem Nath, P.G. Chengappa, Elumalai Kannan, K.R.M. Swamy and C.P.A. Iyer (Eds.). Development Trends in Urban and Peri-urban Agriculture, pp 240, Westville Publishing House, New Delhi. ISBN 978-93-83491-22-3. In press.

Maréchal J.C., Dewandel B., Ahmed S., Galeazzi L., Zaidi F.K. 2006. Combined estimation of specific yield and natural recharge in a semi-arid groundwater basin with irrigated agriculture. Journal of Hydrology 329, 281– 293.

Massuel, S., George, B., Gaur, A., Nune, R. 2007. Groundwater Modelling for Sustainable Resource Management in the Musi Catchment, India. Proceedings, International Congress on Modelling and Simulation, 10-13 December 2007, Christchurch, New Zealand, p. 1429-1435.

McCartney, M., Scott, C., Ensink, J., Jiang, B., Biggs, T. W. 2008. Salinity implications of wastewater irrigation in the Musi River catchment in India. Cey. J. Sci. (Bio. Sci.) 37 (1): 49-59.

Perrin, J., Ahmed, S., Dinis, L., Aellen, V., Amerasinghe, P., Pavelic, P., Schmitt, R. 2011. Groundwater processes in a micro-watershed influenced by wastewater irrigation, peri-urban Hyderabad. National Geophysical Research Institute (NGRI), Bureau de recherches géologiques et minières (BRGM), International Water Management Institute (IWMI). pp 54.

Pettenati, M., Perrin, J., Pauwels, H., Ahmed, S. 2013. Simulating fluoride evolution in groundwater using a reactive multicomponent transient transport model: Application to a crystalline aquifer of Southern India. Applied Geochemistry 29: 102–116.

Schmitt, R. 2010. Wastewater reuse in Indian peri-urban agriculture: Assessment of irrigation practices in a small, peri-urban catchment in Hyderabad, Andhra Pradesh, India. Msc report ETHZ, Zurich.

Theis, CV. 1935. The relation between the lowering of the piezometric surface and the rate and duration of discharge of a well using groundwater storage. Am Geophys Union Trans 16:519-524.

WHO (World Health Organization). 2006. Guidelines for the safe use of wastewater, excreta and greywater. Volume 2: Wastewater use in agriculture. Geneva, Switzerland: WHO.

8 Appendix

8.1 Types of water use in the Kachiwani Singarum micro-watershed.

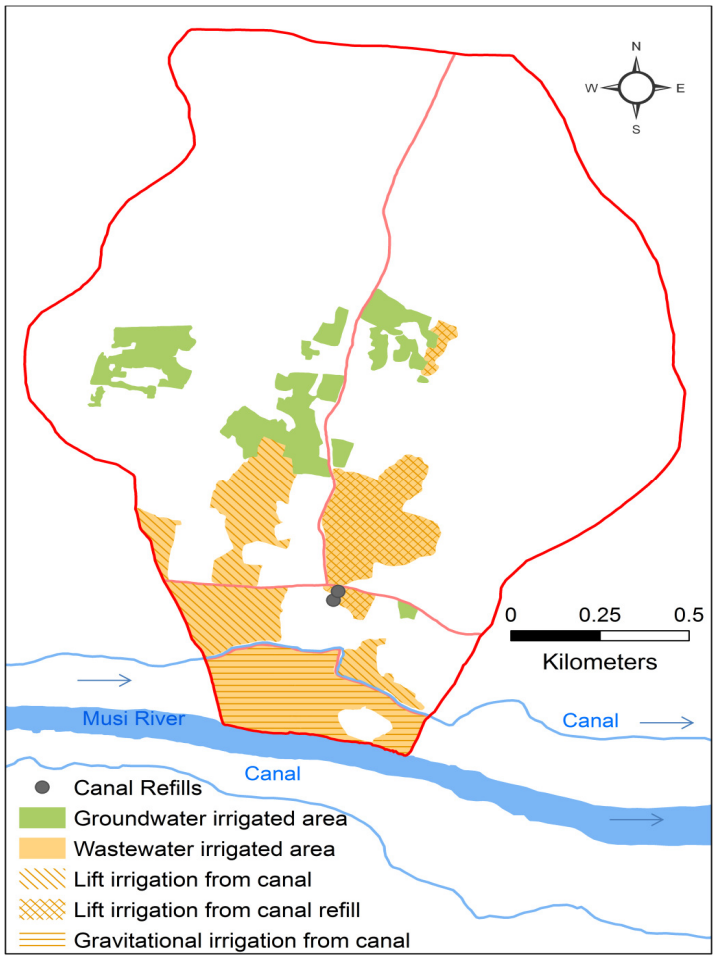

8.2 Soil classification of the study area

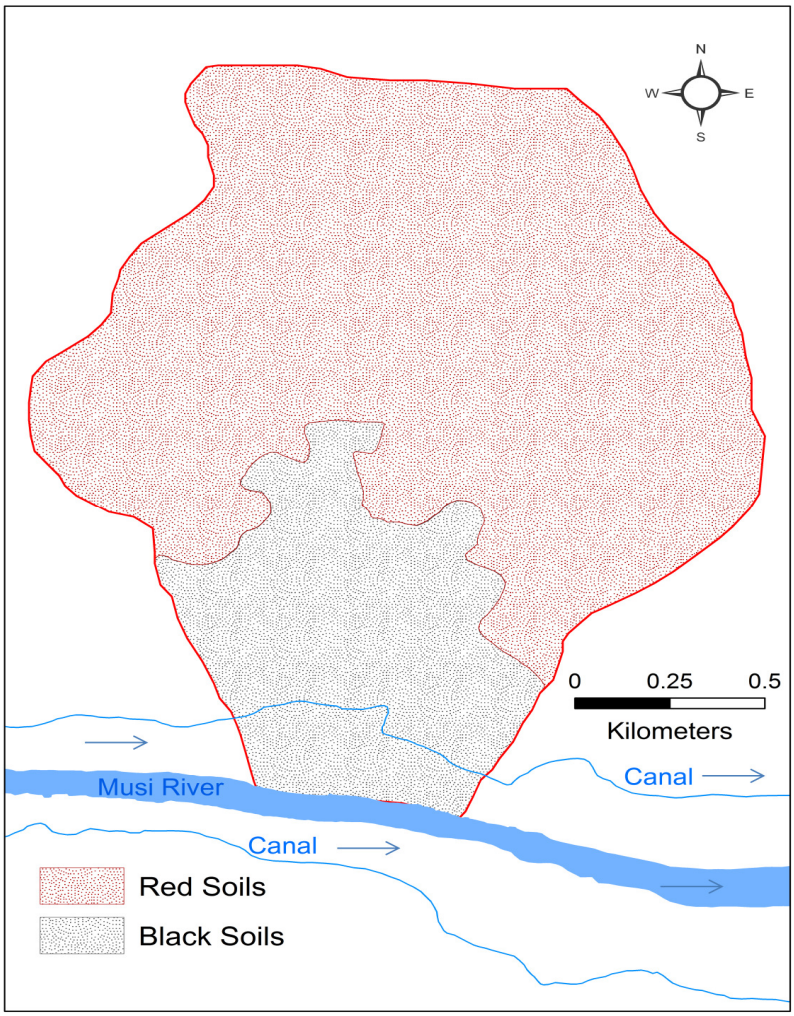

8.3 Peizometric well details

Well ID*	Location	Total depth (m)	Casing + Screen length (m)	Crop Type
MU01 (W1)	Narapally	39	13.4	Paddy
MU02 (W5)	Narapally	65.5	15.2	Paragrass
MU03 (W8)	Narapally	65.5	25.9	Paddy
MU04 (W6)	Narapally	42.5	12.2	Vegetables

8.4 Water quality standards for irrigation purposes

Parameter	Description	Units	Degree of restriction on use		
			None	Slight to Moderate	Severe
Salinity ec_w[1]		Ds/m	<0.7	0.7 – 3.0	>3.0
TDS[1,2]		Mg/L	<450	450 – 2000	>2000
SAR[1,2,3]	0 – 3	Meq/L	>0.7 ec_w	0.7 – 0.2 ec_w	<0.2 ec_w
	3 – 6	Meq/L	>1.2 ec_w	1.2 – 0.3 ec_w	<0.3 ec_w
	6 – 12	Meq/L	>1.9 ec_w	1.9 – 0.5 ec_w	<0.5 ec_w
	12 – 20	Meq/L	>2.9 ec_w	2.9 – 1.3 ec_w	<1.3 ec_w
	20 – 40	Meq/L	>5.0 ec_w	5.0 – 2.9 ec_w	<2.9 ec_w
Sodium (Na^+)[3,4]	Sprinkler irrigation	Meq/L	<3	>3	-
	Surface irrigation	Meq/L	<3	3 – 9	>9
Chloride (Cl^-)[3,4]	Sprinkler irrigation	Meq/L	<3	>3	-
	Surface irrigation	Meq/L	<4	4 – 10	>10
Bicarbonate (HCO_3^-)[2,3]		Mg/L	<90	90 – 500	>500
Nitrogen (NO_3 – N)[2,3]		Mg/L	<5	5 – 30	>30
Ph[1]			Normally 6.5 to 8.0		

Sources: Ayers & Westcot (1985)[1]; Pescod (1992)[2]; Asano & Levine (1998)[3]; WHO (2006)[4]. Ec_w = electrical conductivity, a measure of the water salinity, reported in deci Siemens per metre at 25^{O}C; TDS = means total dissolved solids expressed as mg/L; SAR = Sodium adsorption ratio. Values given are calculated using an equation: NO_3 – N = nitrate nitrogen reported in terms of elemental nitrogen expressed in mg/L.

8.5 Threshold levels of trace elements for crop production

Element	Description	Recommended maximum concentration (mg/L)
Al	Aluminum	5.0
As	Arsenic	0.10
Cd	Cadmium	0.01
Cr	Chromium	0.10
Co	Cobalt	0.05
F	Fluoride	1.0
Fe	Iron	5.0
Li	Lithium	2.5
Mn	Manganese	0.01
Ni	Nickel	0.20
Pb	Lead	5.0
Zn	Zinc	2.0

Sources: Ayers & Westcot (1985); Pescod (1992); WHO (2006).

8.6 Geological log of MU 01

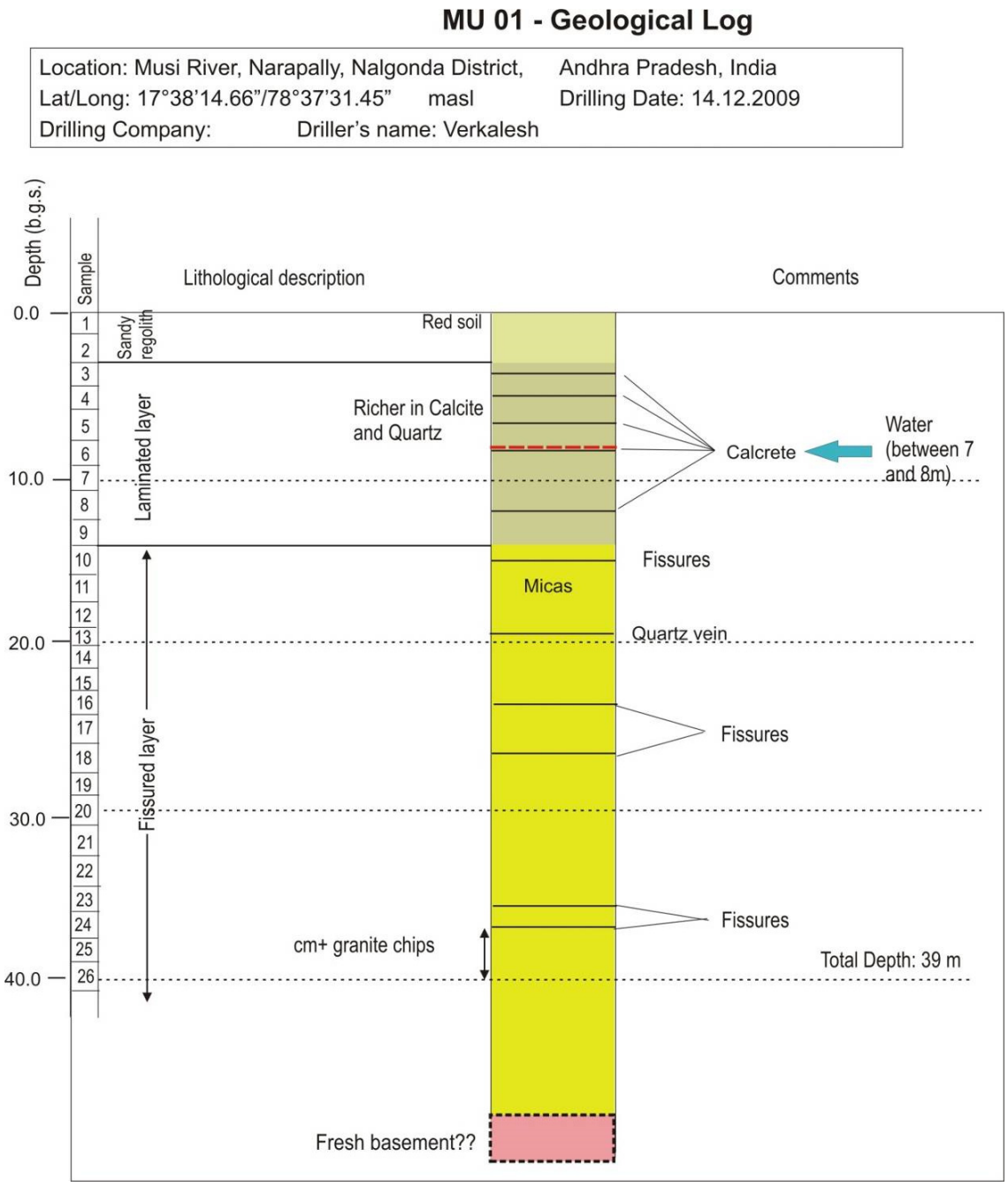

8.7 Geological log of MU 02

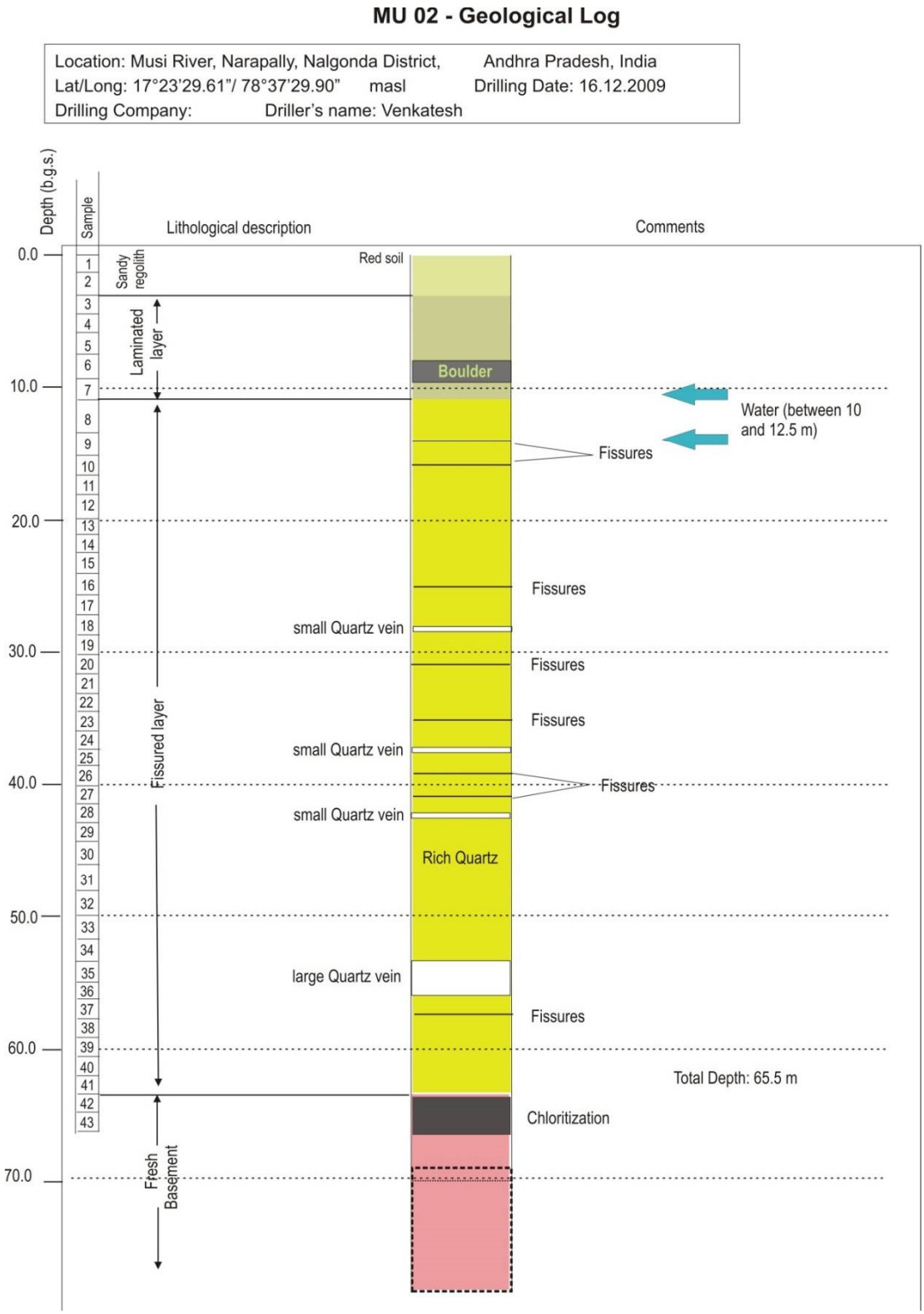

8.8 Geological log of MU 03

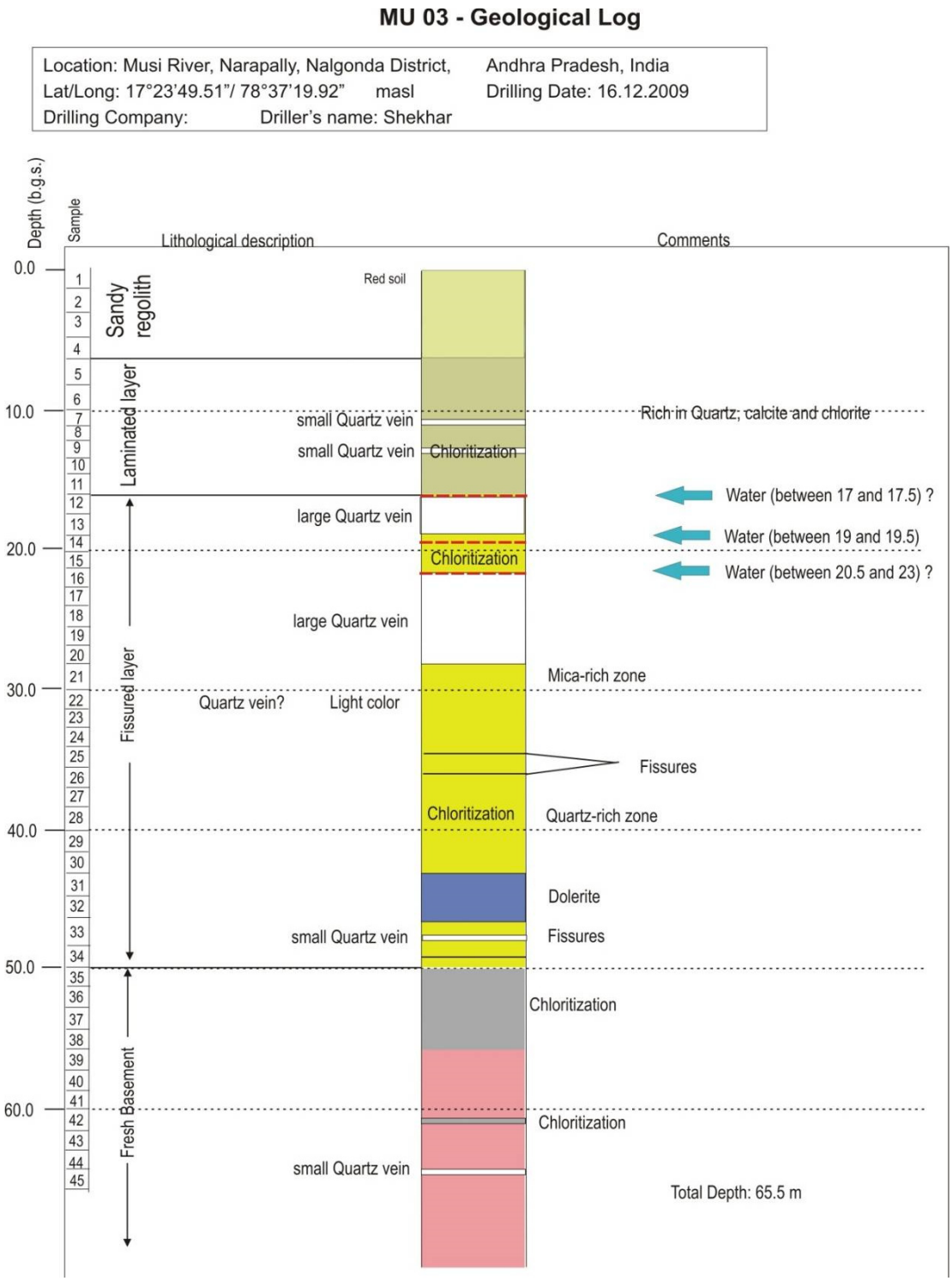

8.9 Geological log of MU 04

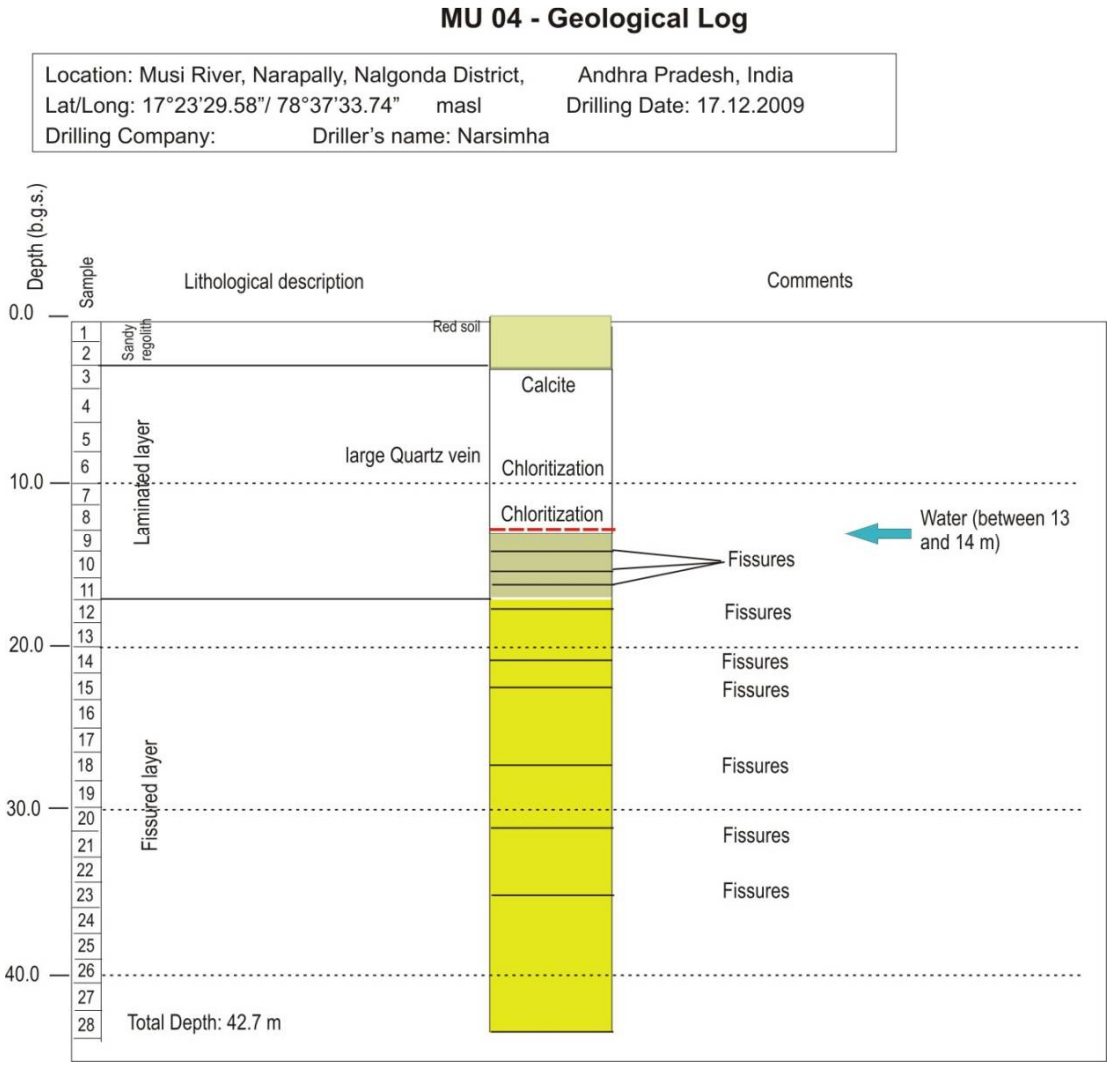

8.9 Details of ERT investigations carried out in Musi River study area, Hyderabad

Longitude	Latitude	ERT No.	ERT Orientation	Electrode Configuration	Location
78.62998776	17.3993605	1	North	Wenner-Schlumberger	West of well DW (Upstream)
78.62927776	17.3980405		South		
78.62866776	17.3975305	2	North	Wenner-Schlumberger	West of well FW-12 (Upstream)
78.62807776	17.3954205		South		
78.62811776	17.3953905	3	North	Wenner-Schlumberger	West of well OW-1 (Mid stream)
78.62782776	17.3933205		South		
78.62822776	17.3916605	4	North	Wenner-Schlumberger	East of MU 02 = W5
78.62795776	17.3895605		South		
78.62322776	17.3959005	5	West	Dipole-Dipole	Near MU 03 = W8
78.62106776	17.3961305		East		
78.62322776	17.3959005	6	West	Wenner-Schlumberger	Near MU 03 = W8
78.62106776	17.3961305		East		
78.62199776	17.3935005	7	North	Wenner-Schlumberger	South of FW (western part of study area)
78.62116776	17.3893705		South		
78.62514776	17.3888305	8	North	Dipole-Dipole	North of CWI (Between road and Canal)
78.62505776	17.3871205		South		
78.62514776	17.3888305	9	North	Wenner-Schlumberger	North of CWI (Between road and Canal)
78.62505776	17.3871205		South		
78.62870776	17.3866805	10	West	Dipole-Dipole	Near CWO (Parallel to Canal)
78.63049776	17.3854505		East		
78.62870776	17.3866805	11	West	Wenner-Schlumberger	Near CWO (Parallel to Canal)
78.63049776	17.3854505		East		
78.62578776	17.3870405	12	North	Dipole-Dipole	Near MU 01 = W1 (Between Canal and Musi River)
78.62564776	17.3864105		South		
78.62578776	17.3870405	13	North	Wenner-Schlumberger	Near MU 01 = W1 (Between Canal and Musi River)
78.62564776	17.3864105		South		
78.62541776	17.3890105	14	North	Dipole-Dipole	Near PW (South of MU 02 = W5)
78.62540776	17.3898605		South		
78.62541776	17.3890105	15	North	Wenner-Schlumberger	Near PW (South of MU 02 = W5)
78.62540776	17.3898605		South		
78.62517776	17.3905105	16	North-West	Dipole-Dipole	Near MU 02 = W5
78.62547776	17.3896905		South-East		
78.62517776	17.3905105	17	North-West	Wenner-Schlumberger	Near MU 02 = W5
78.62547776	17.3896905		South-East		